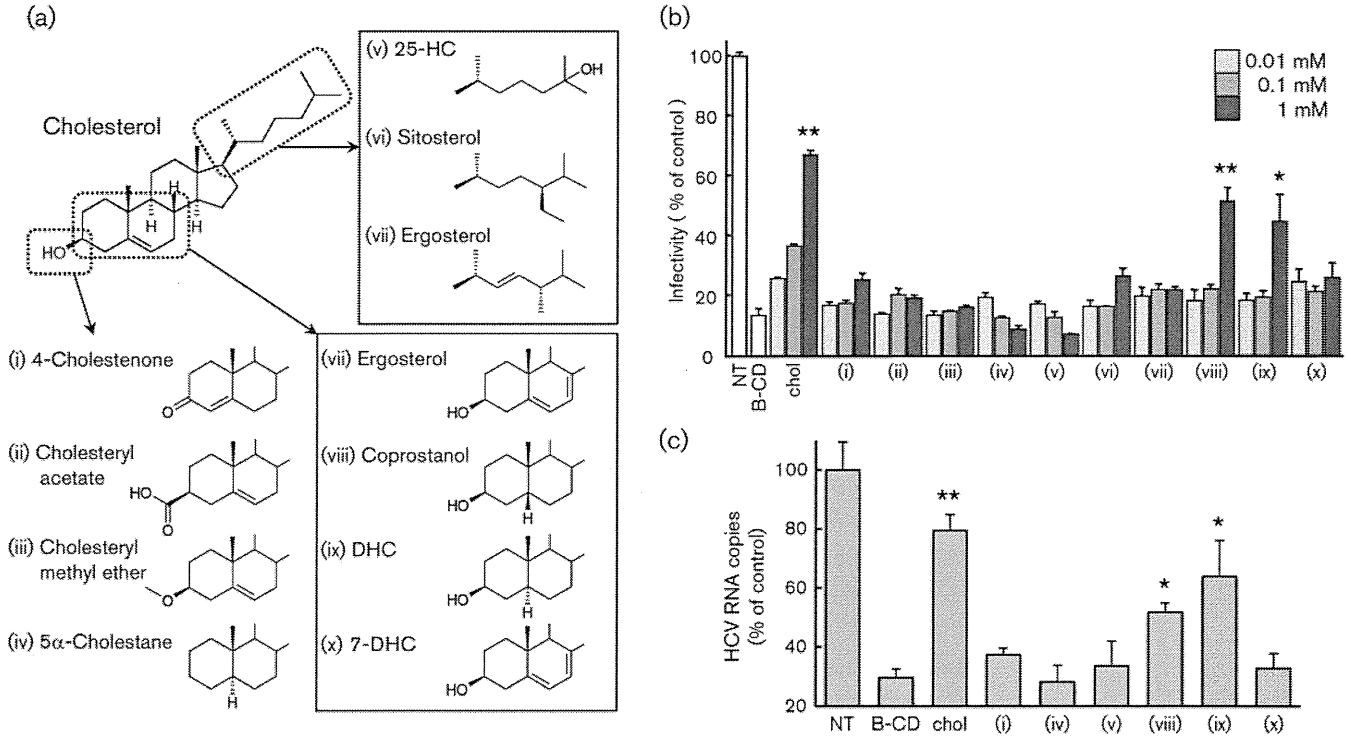

Fig. 1. Role of virion-associated cholesterol analogues in virus infection. (a) Structures of sterols used in this study. Variations in the 3β-hydroxyl group (lower left), aliphatic side chain (upper right) or ring structure (lower right) of cholesterol are shown. (i–x) Compounds studied in (b) and (c). (b) Effect of replenishment with sterols on HCV infectivity. Intracellular HCV core levels were determined at 72 h p.i. as the indicator of infectivity, which is represented as a percentage of the untreated HCVcc level (NT). (c) Effects of virion-associated sterols on virus internalization. HCV RNA copies in cells after virus internalization were quantified and are shown as percentages of the untreated HCVcc level (NT). (b, c) Means+SD of four samples are shown. *P<0.05; **P<0.01, compared with B-CD-treated virus (unpaired Student's t-test). Data are representative of at least two experiments.

recovered by addition of cholesterol at 0.01–1 mM in a dose-dependent manner (Fig. 1b). Among the cholesterol analogues tested, variants with a 3β-hydroxyl group (4-cholestenone, cholesteryl acetate, cholesteryl methyl ether and 5α-cholestane) or variants with an aliphatic side chain [25-hydroxycholesterol (25-HC), sitosterol and ergosterol] exhibited no or little effect on the recovery of infectivity of B-CD-treated HCV (Fig. 1b, lanes i–vii). In contrast, addition of variants in the structure of the sterol rings [coprostanol or dihydrocholesterol (DHC)] at 1 mM restored infectivity to around 50 % compared with non-treated virus control (Fig. 1b, lanes viii and ix). Other variants in the ring structure [7-dehydrocholesterol (7-DHC) and ergosterol, which is also a variant with an aliphatic side chain as indicated above] did not show any increase in the infectivity of B-CD-treated virus (Fig. 1b, lanes x and vii).

We demonstrated previously that HCV-associated cholesterol plays an important role in the internalization step of the virus, but not in cell attachment during virus entry (Aizaki *et al.*, 2008). The effect of virion-associated cholesterol analogues on virus attachment to cells and following internalization was determined. HCVcc, treated with B-CD with or without subsequent replenishment with sterols, was incubated with Huh7-25-CD81 cells, which stably express CD81 (Akazawa *et al.*, 2007), for 1 h at 4 °C. As an internalization assay, the incubation temperature was shifted to 37 °C post-binding procedure and maintained for 2 h. The cells were then treated with 0.25 % trypsin for 10 min at 37 °C, by which >90 % of HCV bound to the cell surface was removed (data not shown; Aizaki *et al.*, 2008). Internalized HCV was quantified by measuring the viral RNA in cell lysates by real-time RT-PCR (Takeuchi *et al.*, 1999). B-CD treatment or supplementation with sterols of B-CD-treated HCV had little or no effect on virus attachment to the cell surface (data not shown). Regarding virus internalization (Fig. 1c), treatment of HCVcc with 1 mM B-CD resulted in approximately 70 % reduction of viral RNA. The reduced level of the internalized HCV recovered markedly to approximately 80 % of the untreated HCVcc level by replenishment with 1 mM cholesterol. In agreement with the results shown in Fig. 1(b), addition of coprostanol or DHC to the B-CD-treated virus caused a significant recovery of virus internalization, suggesting that coprostanol and DHC associated with the

virion have the ability to play a role in HCV internalization into cells, in a manner comparable to cholesterol (Fig. 1c, lanes viii and ix). No or only a little recovery of virus internalization was observed by loading with other cholesterol analogues, such as 4-cholestenone, 5α-cholestane, 25-HC or 7-DHC (Fig. 1c, lanes i, iv, v and x).

To monitor the effect of cholesterol analogues on the physical characteristics of HCV, we next investigated buoyant-density profiles by using sucrose density-gradient centrifugation, in which untreated, B-CD-treated and sterol-replenished HCVcc were concentrated and layered onto continuous 10–60 % (w/v) sucrose density gradients, followed by centrifugation at 35 000 r.p.m. (151 000 *g*) for 14 h. Fractions were collected and analysed for the core protein. Fig. 2 shows that the virus density became higher after treatment with B-CD and that cholesterol-replenished virus shifted the density of B-CD-treated HCV to the non-treated level. Consistent with the result shown in Fig. 1(b), no effect on restoration of the buoyant densities of HCV was observed using variants with modifications in either the 3β-hydroxyl group (4-cholestenone, cholesteryl acetate and 5α-cholestane) or the aliphatic side chain (25-HC and sitosterol). In contrast, variants in the sterol ring structure (coprostanol, DHC and 7-DHC) had an ability to recover the density of B-CD-treated virus to that of non-treated virus.

Incorporation efficiency of the sterols into the cholesterol-depleted HCVcc was further determined by gas chromatography with flame ionization detection (see Supplementary Table S1, available in JGV Online). Under the experimental conditions used, exogenously supplied cholesterol after B-CD treatment was able to restore cholesterol content in HCVcc almost to initial levels. When 4-cholestenone, cholesteryl acetate, 25-HC, DHC or 7-DHC was added to B-CD-treated HCVcc, virion-associated sterol levels were 146, 157, 68, 96 or 73 %, respectively, of that of the non-treated control. The proportion of cholesterol analogues to the total sterols incorporated was ⩾30 % when 4-cholestenone, cholesteryl acetate, DHC or 7-DHC was used; however, the proportion in the case of 25-HC was only 3 %. It may be that the hydrophilic modification of the aliphatic side chain leads to poor association with HCVcc.

Collectively, exogenous variants with the 3β-hydroxyl group, such as 4-cholestenone and cholesteryl acetate, can be incorporated into B-CD-treated HCVcc, but resulted in no recovery of virus infectivity, indicating the importance of the 3β-hydroxyl group of cholesterol associated with the virus envelope in HCV infectivity. In contrast, two variants with modification in their sterol ring structures, coprostanol and DHC, have the ability to substitute for cholesterol. However, 7-DHC, another variant within the sterol ring, is incorporated readily into the depleted virion and restores the virus density, HCV replenished with 7-DHC is not infectious. These facts suggest that reduced forms of the sterol ring (coprostanol and DHC) in virion-associated cholesterol can be permitted for maintaining virus infectivity. However, a molecule with an additional double bond in the ring structure (7-DHC) seems to fail to exhibit infectivity, presumably because the change reduces structural flexibility in the

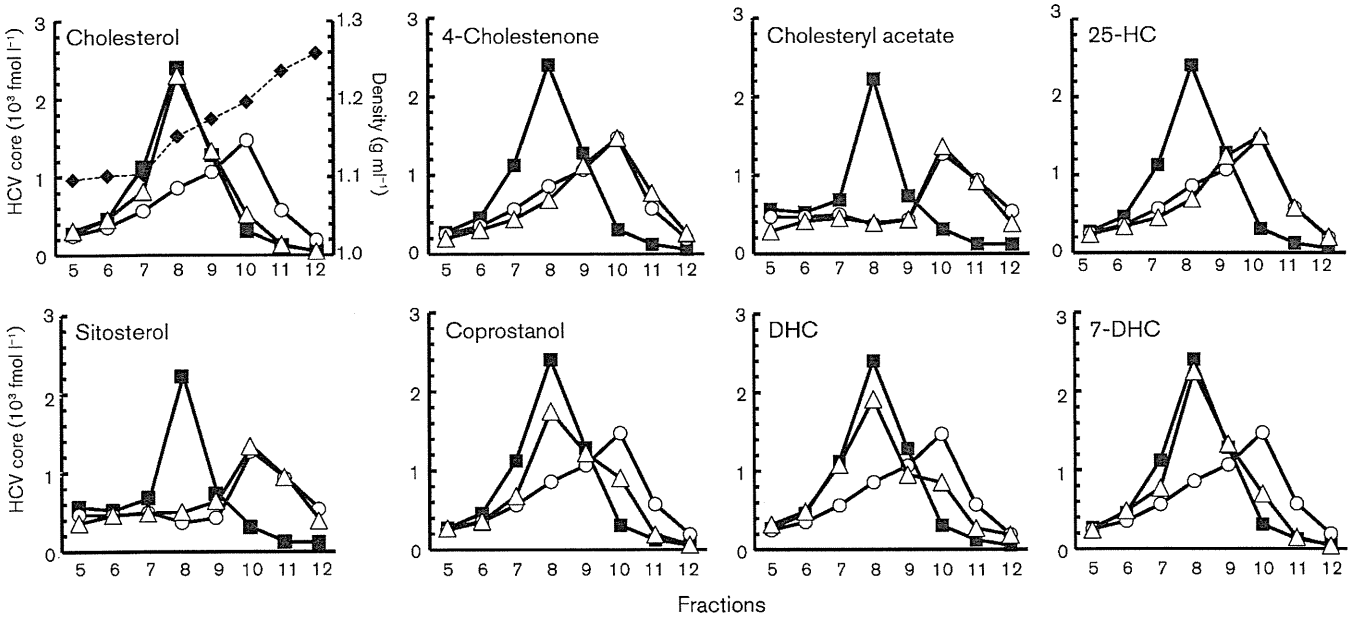

Fig. 2. Sucrose density-gradient profiles of lipid-modified HCV. Core protein concentration in each fraction of untreated HCVcc (■), B-CD-treated HCVcc (○) or HCVcc replenished with sterols (△) was determined. Corresponding densities of fractions are shown as a dashed line (◆).

sterol molecule and consequently in the virion structure. Coprostanol and DHC are *cis* and *trans* isomers, which are often known to have different physical properties. However, based on their molecular models, these two sterols, as well as cholesterol, possibly have similar spatial arrangements of the aliphatic side chain, the hydroxyl group and four-ring region because of their structural flexibility. In contrast, the spatial arrangement of 7-DHC does not seem comparable to that of cholesterol. Campbell *et al.* (2004) reported that replacement of HIV-1-associated cholesterol with raft-inhibiting sterols, including coprostanol, suppresses HIV-1 infectivity, whereas replacement with raft-promoting analogues such as DHC and 7-DHC (Megha *et al.*, 2006; Wang *et al.*, 2004; Xu & London, 2000; Xu *et al.*, 2001) maintains infectivity, demonstrating the importance of the raft-promoting properties of virion-associated cholesterol in HIV-1 infectivity (Campbell *et al.*, 2004). It is therefore likely that HCV-associated cholesterol is involved, at least in part, in virus infectivity via a molecular basis independent of lipid-raft formation.

The density of blood-circulating HCV is heterogeneous, ranging approximately from <1.06 to 1.25 g ml^{-1}, and it is proposed that low-density virus is associated with very-low-density lipoprotein (VLDL) and/or low-density lipoprotein (LDL) (André *et al.*, 2002; Thomssen *et al.*, 1993). It has recently been demonstrated that the pathway for VLDL assembly plays a role in assembly and maturation of infectious HCVcc (Icard *et al.*, 2009). HCVcc with low density, which is presumably associated with VLDL or VLDL-like lipoproteins, was found to possess higher infectivity than that with high density (Lindenbach *et al.*, 2006). This study, as well as our earlier work, indicated that removal of cholesterol from HCVcc by B-CD increased the buoyant density of the virus and reduced its infectivity. Thus, one may hypothesize that the virion-associated cholesterol plays a role in the formation of a complex with lipoproteins or apolipoproteins. To address this, the interaction between apolipoproteins and HCVcc with or without B-CD treatment was investigated by co-immunoprecipitation (Co-IP kit; Thermo Scientific). Virus samples were subjected separately to AminoLink Plus coupling resin, which was conjugated with a monoclonal antibody (mAb) against apolipoprotein E (ApoE) or apolipoprotein B (ApoB), and incubated at 4 °C for 4 h. After washing, total RNAs were extracted from the resulting resin beads by using TRIzol reagent (Invitrogen), followed by quantification of HCV RNA as described above (Takeuchi *et al.*, 1999). As indicated in Fig. 3(a), only a fraction of HCVcc was precipitated with an anti-ApoB mAb. In contrast, an anti-ApoE mAb was able to coprecipitate a considerable amount of the virus. It is of interest that B-CD-treated HCVcc hardly reacted with the mAb; however, the cholesterol-replenished virus was found to recover its reactivity, suggesting a role for virion-associated cholesterol in the formation of the HCV–lipoprotein/apolipoprotein complex. The results obtained are consistent with findings indicating that HCVcc can be captured with anti-ApoE antibodies, but capture with anti-ApoB antibodies is inefficient (Chang *et al.*, 2007; Hishiki *et al.*, 2010; Huang *et al.*, 2007; Jiang & Luo, 2009; Merz *et al.*, 2011; Nielsen *et al.*, 2006; Owen *et al.*, 2009), as well as with a recent model of structures of infectious HCV, in which HCVcc looks like ApoE-positive and primarily ApoB-negative lipoproteins (Bartenschlager *et al.*, 2011). We further tested the ApoE distribution in the density-gradient fractions of HCVcc samples (see Supplementary Fig. S1, available in JGV Online). With or without cholesterol depletion, ApoE was detected at a wide range of concentrations: 1.04 g ml^{-1} (fraction 1) to 1.17 g ml^{-1} (fraction 9). However, its level in the fractions at 1.10 g ml^{-1} (fraction 5) to approximately 1.17 g ml^{-1} was moderately decreased in the case of B-CD-treated virus.

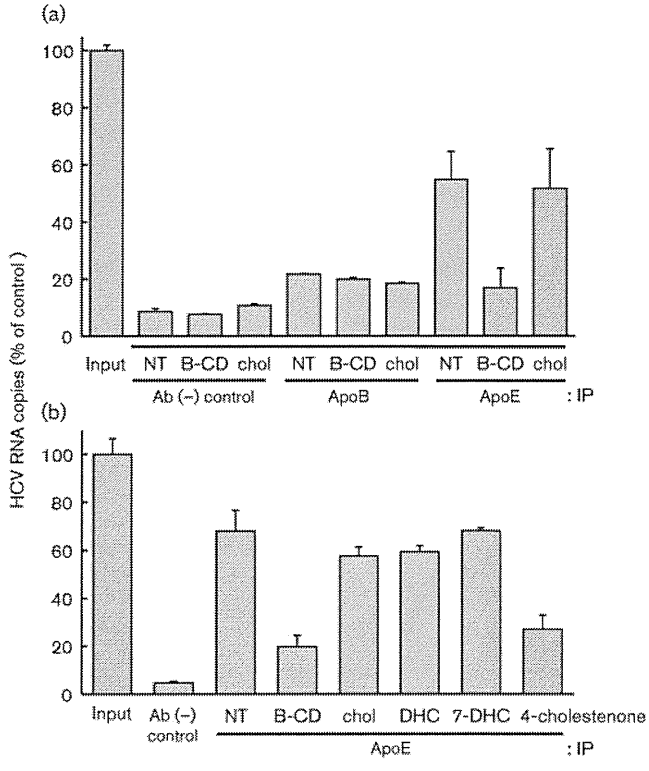

Fig. 3. Effect of virion-associated sterols on HCV–apolipoprotein interaction. (a) HCVcc samples with no treatment (NT), B-CD-treated (B-CD) or replenished with cholesterol (chol) were incubated with an amine-reactive resin coupling either an anti-ApoB mAb (ApoB) or an anti-ApoE mAb (ApoE). Control resin that is composed of the same material as above, but is not activated, was used as a negative control [Ab (–) control]. (b) B-CD-treated HCVcc was incubated with cholesterol (chol), DHC, 7-DHC or 4-cholestenone, followed by immunoprecipitation with the resin coupling with anti-ApoE mAb. (a, b) HCV RNAs in the immunoprecipitates were quantified and are indicated as percentages of the amount of input HCVcc RNA. Means+SD of three samples are shown. Data are representative of three experiments.

Whether cholesterol analogues could have a comparable role in HCV association with lipoprotein was examined further (Fig. 3b). Addition of DHC or 7-DHC, but not 4-cholestenone, to B-CD-treated HCVcc resulted in the recovery of coprecipitation of the virus with anti-ApoE. The results are correlated with the effect of sterols on the restoration of the buoyant densities of lipid-modified HCVcc (Fig. 2), suggesting that virion-associated cholesterol variants with modification in the sterol rings, but not in either the 3β-hydroxyl group or the aliphatic side chain, may tolerate the interaction between HCV and ApoE-positive lipoprotein.

Given that 7-DHC restored the association of HCV with ApoE and virion buoyant density, but did not restore infectivity, cholesterol and/or its analogues might affect the ability of virion membranes to fuse with the cell, independent of ApoE association. As cholesterol is an important mediator of membrane fluidity, one may hypothesize that HCV-associated cholesterol is involved in infectivity through modulation of the membrane fluidity. It has been reported that, in patients with Smith–Lemli–Opitz syndrome, a disorder of the cholesterol-synthesis pathway, cholesterol content decreases and 7-DHC increases in the cell membranes, leading to alteration of phospholipid packing in the membrane and abnormal membrane fluidity (Tulenko *et al.*, 2006).

It is now accepted that maturation and release of infectious HCV coincide with the pathway for producing VLDLs, which export cholesterol and triglyceride from hepatocytes. This study revealed roles for the structural basis of virion-associated cholesterol in the infectivity, buoyant density and apolipoprotein association of HCV. Although it was shown that HCV virions in infected patients, so-called lipo–viro particles, exhibited certain biochemical properties such as containing ApoB, ApoC and ApoE (Diaz *et al.*, 2006; Bartenschlager *et al.*, 2011), our studies provide useful information and the basis for future investigations toward a deeper understanding of the biogenesis pathway of infectious HCV particles.

Acknowledgements

We thank M. Matsuda, M. Sasaki and T. Date for technical assistance and T. Mizoguchi for secretarial work. This work was partially supported by a grant-in-aid for Scientific Research from the Japan Society for the Promotion of Science, from the Ministry of Health, Labor, and Welfare of Japan, and from the Ministry of Education, Culture, Sports, Science, and Technology.

References

Aizaki, H., Morikawa, K., Fukasawa, M., Hara, H., Inoue, Y., Tani, H., Saito, K., Nishijima, M., Hanada, K. & other authors (2008). Critical role of virion-associated cholesterol and sphingolipid in hepatitis C virus infection. *J Virol* **82**, 5715–5724.

Akazawa, D., Date, T., Morikawa, K., Murayama, A., Miyamoto, M., Kaga, M., Barth, H., Baumert, T. F., Dubuisson, J. & Wakita, T. (2007). CD81 expression is important for the permissiveness of Huh7 cell clones for heterogeneous hepatitis C virus infection. *J Virol* **81**, 5036–5045.

André, P., Komurian-Pradel, F., Deforges, S., Perret, M., Berland, J. L., Sodoyer, M., Pol, S., Bréchot, C., Paranhos-Baccalà, G. & Lotteau, V. (2002). Characterization of low- and very-low-density hepatitis C virus RNA-containing particles. *J Virol* **76**, 6919–6928.

Bartenschlager, R., Penin, F., Lohmann, V. & André, P. (2011). Assembly of infectious hepatitis C virus particles. *Trends Microbiol* **19**, 95–103.

Bremer, C. M., Bung, C., Kott, N., Hardt, M. & Glebe, D. (2009). Hepatitis B virus infection is dependent on cholesterol in the viral envelope. *Cell Microbiol* **11**, 249–260.

Campbell, S. M., Crowe, S. M. & Mak, J. (2001). Lipid rafts and HIV-1: from viral entry to assembly of progeny virions. *J Clin Virol* **22**, 217–227.

Campbell, S. M., Crowe, S. M. & Mak, J. (2002). Virion-associated cholesterol is critical for the maintenance of HIV-1 structure and infectivity. *AIDS* **16**, 2253–2261.

Campbell, S., Gaus, K., Bittman, R., Jessup, W., Crowe, S. & Mak, J. (2004). The raft-promoting property of virion-associated cholesterol, but not the presence of virion-associated Brij 98 rafts, is a determinant of human immunodeficiency virus type 1 infectivity. *J Virol* **78**, 10556–10565.

Chang, K. S., Jiang, J., Cai, Z. & Luo, G. (2007). Human apolipoprotein E is required for infectivity and production of hepatitis C virus in cell culture. *J Virol* **81**, 13783–13793.

Diaz, O., Delers, F., Maynard, M., Demignot, S., Zoulim, F., Chambaz, J., Trépo, C., Lotteau, V. & André, P. (2006). Preferential association of hepatitis C virus with apolipoprotein B48-containing lipoproteins. *J Gen Virol* **87**, 2983–2991.

Graham, D. R., Chertova, E., Hilburn, J. M., Arthur, L. O. & Hildreth, J. E. (2003). Cholesterol depletion of human immunodeficiency virus type 1 and simian immunodeficiency virus with β-cyclodextrin inactivates and permeabilizes the virions: evidence for virion-associated lipid rafts. *J Virol* **77**, 8237–8248.

Hambleton, S., Steinberg, S. P., Gershon, M. D. & Gershon, A. A. (2007). Cholesterol dependence of varicella-zoster virion entry into target cells. *J Virol* **81**, 7548–7558.

Hishiki, T., Shimizu, Y., Tobita, R., Sugiyama, K., Ogawa, K., Funami, K., Ohsaki, Y., Fujimoto, T., Takaku, H. & other authors (2010). Infectivity of hepatitis C virus is influenced by association with apolipoprotein E isoforms. *J Virol* **84**, 12048–12057.

Huang, H., Sun, F., Owen, D. M., Li, W., Chen, Y., Gale, M., Jr & Ye, J. (2007). Hepatitis C virus production by human hepatocytes dependent on assembly and secretion of very low-density lipoproteins. *Proc Natl Acad Sci U S A* **104**, 5848–5853.

Icard, V., Diaz, O., Scholtes, C., Perrin-Cocon, L., Ramière, C., Bartenschlager, R., Penin, F., Lotteau, V. & André, P. (2009). Secretion of hepatitis C virus envelope glycoproteins depends on assembly of apolipoprotein B positive lipoproteins. *PLoS One* **4**, e4233.

Jiang, J. & Luo, G. (2009). Apolipoprotein E but not B is required for the formation of infectious hepatitis C virus particles. *J Virol* **83**, 12680–12691.

Lindenbach, B. D., Meuleman, P., Ploss, A., Vanwolleghem, T., Syder, A. J., McKeating, J. A., Lanford, R. E., Feinstone, S. M., Major, M. E. & other authors (2006). Cell culture-grown hepatitis C virus is infectious *in vivo* and can be recultured *in vitro*. *Proc Natl Acad Sci U S A* **103**, 3805–3809.

Megha, Bakht, O. & London, E. (2006). Cholesterol precursors stabilize ordinary and ceramide-rich ordered lipid domains (lipid

rafts) to different degrees. Implications for the Bloch hypothesis and sterol biosynthesis disorders. *J Biol Chem* **281**, 21903–21913.

Merz, A., Long, G., Hiet, M. S., Brügger, B., Chlanda, P., Andre, P., Wieland, F., Krijnse-Locker, J. & Bartenschlager, R. (2011). Biochemical and morphological properties of hepatitis C virus particles and determination of their lipidome. *J Biol Chem* **286**, 3018–3032.

Nielsen, S. U., Bassendine, M. F., Burt, A. D., Martin, C., Pumeechockchai, W. & Toms, G. L. (2006). Association between hepatitis C virus and very-low-density lipoprotein (VLDL)/LDL analyzed in iodixanol density gradients. *J Virol* **80**, 2418–2428.

Owen, D. M., Huang, H., Ye, J. & Gale, M., Jr (2009). Apolipoprotein E on hepatitis C virion facilitates infection through interaction with low-density lipoprotein receptor. *Virology* **394**, 99–108.

Takeuchi, T., Katsume, A., Tanaka, T., Abe, A., Inoue, K., Tsukiyama-Kohara, K., Kawaguchi, R., Tanaka, S. & Kohara, M. (1999). Real-time detection system for quantification of hepatitis C virus genome. *Gastroenterology* **116**, 636–642.

Thomssen, R., Bonk, S. & Thiele, A. (1993). Density heterogeneities of hepatitis C virus in human sera due to the binding of beta-lipoproteins and immunoglobulins. *Med Microbiol Immunol (Berl)* **182**, 329–334.

Tulenko, T. N., Boeze-Battaglia, K., Mason, R. P., Tint, G. S., Steiner, R. D., Connor, W. E. & Labelle, E. F. (2006). A membrane defect in the pathogenesis of the Smith–Lemli–Opitz syndrome. *J Lipid Res* **47**, 134–143.

Wakita, T., Pietschmann, T., Kato, T., Date, T., Miyamoto, M., Zhao, Z., Murthy, K., Habermann, A., Kräusslich, H. G. & other authors (2005). Production of infectious hepatitis C virus in tissue culture from a cloned viral genome. *Nat Med* **11**, 791–796.

Wang, J., Megha & London, E. (2004). Relationship between sterol/steroid structure and participation in ordered lipid domains (lipid rafts): implications for lipid raft structure and function. *Biochemistry* **43**, 1010–1018.

Xu, X. & London, E. (2000). The effect of sterol structure on membrane lipid domains reveals how cholesterol can induce lipid domain formation. *Biochemistry* **39**, 843–849.

Xu, X., Bittman, R., Duportail, G., Heissler, D., Vilcheze, C. & London, E. (2001). Effect of the structure of natural sterols and sphingolipids on the formation of ordered sphingolipid/sterol domains (rafts). Comparison of cholesterol to plant, fungal, and disease-associated sterols and comparison of sphingomyelin, cerebrosides, and ceramide. *J Biol Chem* **276**, 33540–33546.

Vaccine 29 (2011) 4821–4828

Contents lists available at ScienceDirect

Vaccine

journal homepage: www.elsevier.com/locate/vaccine

Production and characterization of HCV particles from serum-free culture

Daisuke Akazawa[a,b], Kenichi Morikawa[b,1], Noriaki Omi[a,b], Hitoshi Takahashi[a,b,2], Noriko Nakamura[a], Hidenori Mochizuki[a], Tomoko Date[b], Koji Ishii[b], Tetsuro Suzuki[b,3], Takaji Wakita[b,*]

[a] *Pharmaceutical Research Laboratories, Toray Industries, Inc., Kanagawa, Japan*
[b] *Department of Virology II, National Institute of Infectious Diseases, 1-23-1 Toyama, Shinjuku-ku, Tokyo, Japan*

ARTICLE INFO

Article history:
Received 26 October 2010
Received in revised form 8 April 2011
Accepted 19 April 2011
Available online 7 May 2011

Keywords:
Hepatitis C virus
Cell culture
Serum-free
Apolipoprotein

ABSTRACT

Hepatitis C virus (HCV) is a major cause of liver cancer, and it is therefore important to develop a prophylactic strategy for HCV infection. In recent years, a system for cell culture of the infectious HCV particle has been established, and the inactivated particle has potential as an antigen for vaccine development. In this study, we aimed to establish highly efficient HCV particle purification procedures using the following serum-free culture of HCV particles. First, naïve human hepatoma Huh7 cells were grown in serum-free medium that was supplemented with human-derived insulin, transferrin and sodium selenite. Then, *in vitro* transcribed JFH-1 or J6/JFH-1 chimeric HCV-RNA was transfected into the serum-free conditioned Huh7 cells. Infectious HCV was secreted into the culture supernatant with the same efficiency as that from cells cultured in FBS-containing medium. The HCV-core protein and RNA continued to be detected in the culture supernatant when the infected cells were subcultured in serum-free medium. Sucrose gradient centrifugation analyses indicated that the profiles of HCV-core, HCV-RNA and the infectivity of HCV particles were almost identical between HCV from FBS-supplemented and serum-free cultures. We further determined that anti-CD81, anti-SR-BI and anti-E2 antibodies inhibited infection by serum-free cultured HCV to a greater extent than infection by HCV from FBS-supplemented cultures. These HCV particles also differed in the level of associated apoplipoproteins: the ApoE level was lower in serum-free cultured HCV. ApoB and ApoE antibody-depletion assays suggested that infection of serum-free cultured HCV was independent of ApoB and ApoE proteins. These data suggest that lipids conjugated with HCV affect infection and neutralization.

1. Introduction

Hepatitis C virus (HCV) is an enveloped virus that belongs to the *Hepacivirus* genus of the *Flaviviridae* family. HCV is a human pathogen that is a major cause of chronic hepatitis, liver cirrhosis and hepatic carcinoma. HCV therapy mainly involves treatment with pegylated-interferon and rivabirin; however, these agents are not very effective for patients with high titer HCV-RNA and genotype 1. Thus, it is necessary to develop new, more effective therapies and preventive care treatments for HCV. It was discovered that a genotype 2a strain, JFH-1, efficiently replicated in Huh7 cells [1]. Moreover, an *in vitro* culture system that generates infectious HCV has also been successfully developed using the JFH-1 genome [2–4]. Recently, it has been shown to be possible to produce various chimeric HCVs by replacement of the JFH-1 structural protein region with the same region from other strains [5]. These chimeric HCV particles are expected to lead to a HCV vaccine as well as to new pharmaceuticals.

Huh7 is a human hepatoma cell line that was established in 1982 [6]. This cell line can be cultured in serum-free medium supplemented with selenium. Serum-free culture has advantages for the simple purification and preparation of animal-origin-free virus particles. In this study, we successfully produced HCV particles in serum-free culture and compared the properties of these particles to those from FBS-supplemented cultures. Interestingly, serum-free cultured HCV was susceptible to CD81-, SR-BI- and HCV-E2-neutralizing antibodies. It was recently suggested that HCV particles associate with lipids to form viro-lipo particles [7–9], and it has also been shown that HCV particles can associate with

Abbreviations: HCV, hepatitis C virus; ITS, insulin-transferrin-selenium; MOI, multiplicity of infection; MTS, 3-(4,5-dimethylthiazol-2-yl)-5-(3-carboxymethoxyphenyl)-2-(4-sulfophenyl)-2H-tetrazolium; VLDL, very-low-density lipoprotein.

* Corresponding author. Tel.: +81 3 5285 1111; fax: +81 3 5285 1161.
E-mail address: wakita@nih.go.jp (T. Wakita).
[1] Present address: Institute of Microbiology, University of Lausanne, and Division of Gastroenterology and Hepatology, Centre Hospitalier Universitaire Vaudois, Lausanne, Switzerland.
[2] Present address: Center for Influenza Virus Research, National Institute of Infectious Diseases, Tokyo, Japan.
[3] Present address: Department of Infectious Diseases, Hamamatsu University School of Medicine, Hamamatsu, Japan.

0264-410X/$ – see front matter © 2011 Elsevier Ltd. All rights reserved.
doi:10.1016/j.vaccine.2011.04.069

lipids to form exosomes [10,11]. We examined apolipoprotein association of serum-free cultured HCV. We found that this virus had a lower ApoE level than HCV from serum-supplemented cultures and that infection by this virus was apolipoprotein-independent.

2. Materials and methods

2.1. Cell culture

Huh7, Huh7.5.1 ([4], a generous gift from Dr. Francis V. Chisari), Huh7-25 and Huh7-25-CD81 [12] cell lines were cultured in 5% CO_2 at 37 °C in Dulbecco's modified Eagle's medium (DMEM) containing 10% fetal bovine serum (DMEM-10). Our previous FACS analysis indicated that Huh7-25 cells do not express CD81, and that Huh7-25-CD81 constitutively express CD81, on the cell surface [12]. For serum-free culture, the cells were conditioned and cultured in DMEM/F-12 supplemented with Insulin-Transferrin-Selenium-X (ITS) (Invitrogen, Carlsbad, CA).

2.2. Establishment of serum-free cultured cells

Sub-confluent Huh7 cells that were cultured in DMEM-10 were passaged in 10-cm dishes (Nunc, Rochester, NY) in DMEM containing 5% FBS. The cells were then sequentially passaged in DMEM containing 2, 1 and 0.5% FBS and were ultimately passaged in serum-free medium. The cells were detached for passage in serum-free culture using TrypLE Sellect (Invitrogen).

2.3. Cell growth assay

Cell growth was assayed by MTS (3-(4,5-dimethylthiazol-2-yl)-5-(3-carboxymethoxyphenyl)-2-(4-sulfophenyl)-2H-tetrazolium) assay using the CellTiter 96® AQ_{ueous} One Solution Cell Proliferation Assay kit (Promega, Madison, WI) according to the manufacturer's instructions. In brief, 1×10^4 cells were seed into a 96-well culture plate (IWAKI, Tokyo, Japan) in 100 μL of media, and 20 μL of the assay solution was added into each well at the appropriate time. After incubation for 1 h at 37 °C, the absorbance of the solution at 490 nm was measured.

2.4. Plasmids

pJFH1 and pJ6/JFH1 were generated as previously reported [2,13].

2.5. RNA synthesis

RNA synthesis was performed as described previously [14]. Briefly, the pJFH1 and pJ6/JFH1 plasmids were digested with *Xba* I and were treated with Mung Bean nuclease (New England Biolabs, Beverly, MA). The digested plasmid DNA fragment was then purified and was used as a template for RNA synthesis. HCV-RNA was synthesized *in vitro* using a MEGAscript™ T7 kit (Ambion, Austin, TX). The synthesized RNA was treated with DNaseI, followed by acid phenol extraction to remove any remaining template DNA.

2.6. RNA transfection

RNA transfection was performed as described previously [15]. Briefly, trypsinized cells were washed with Opti-MEM I™ reduced-serum medium (Invitrogen) and were resuspended at a density of 7.5×10^6 cells/mL in Cytomix buffer [1]. RNA (10 μg) that was synthesized from pJFH1 or pJ6/JFH1 was mixed with 400 μL of the cell suspension and was transferred into an electroporation cuvette (Precision Universal Cuvettes, Thermo Hybrid, Middlesex, UK). The cells were then pulsed at 260 V and 950 μF with the Gene Pulser II™ apparatus (Bio-Rad, Hercules, CA). Transfected cells were immediately transferred to a 6-well plate, in which each well contained 3 mL of culture medium.

2.7. Infectivity titration

Huh7.5.1 cells were employed to determine the infectivity titer using end point dilution and immunofluorescence as described below. Briefly, each sample was serially diluted 5-fold in DMEM-10 and a 100-μL aliquot was used to inoculate Huh7.5.1 cells. Infection was examined 72 h post-inoculation by immunofluorescence using a mouse monoclonal anti-Core antibody 2H9 and Alexa 488-conjugated secondary anti-mouse IgG antibody. The infectious foci were counted. The titer was then calculated and is indicated as focus forming units per mL (FFU/mL).

2.8. HCV inhibition assay

To analyze the inhibitory effects of anti-CD81 and anti-SR-BI against virus infection, naïve Huh7.5.1 cells (2×10^4) were seeded into a 48-well plate and were incubated for 1 h at 37 °C with JS-81 or rat anti-SR-BI serum ([16], a generous gift from Dr. H. Barth) that was serially diluted with DMEM. Mouse IgG1 (Sigma, St. Louis, MO) and rat pre-immune serum were used as controls for JS-81 and anti-SR-BI, respectively. Antibodies were removed and the cells were washed once with PBS. The cells were then inoculated with viruses (MOI 0.1) from FBS-supplemented or serum-free culture for 3 h, and were then washed with PBS and cultured with DMEM-10 for 72 h. The cells were washed three times with PBS and 100 μL of Passive Lysis Buffer (Promega) was added into each well. Cell lysates were collected and HCV-core concentrations were measured as described below.

To analyze the inhibitory effects of anti-E2 against HCV particles, viruses that were purified from FBS-supplemented or serum-free culture (2×10^3 FFU) were mixed with mouse anti-E2 (AP33, a kind gift from Genentech, Inc.) antibody, and were then incubated for 30 min at room temperature. Naïve Huh7.5.1 cells (1×10^4) were seeded into a poly-D-lysine coated 96-well plate, and cells were inoculated with the virus-antibody mixtures, which were serially diluted with DMEM-10, and, after 3 h, the mixtures were removed and the cells were washed once with PBS. DMEM-10 was added into each well, and the cells were cultured for 72 h. The cells were fixed with methanol for 15 min at −20 °C, and the infected cells were stained with rabbit anti-NS5A antibody using immunofluorescence as described above [17]. Percentage infection was calculated from the infectious titer of each diluted virus.

2.9. Sucrose density gradient analysis and HCV purification

Supernatants (4 mL) of J6/JFH-1 HCV cells were layered on top of a preformed continuous 10–60% sucrose gradient in 10 mM Tris, 150 mM NaCl, and 0.1 mM EDTA (TNE buffer). HCV-core levels, HCV-RNA titer and infectious titers of the media are shown in the supplementary table. The gradients were centrifuged using an SW41 rotor (Beckman Coulter, Fullerton, CA) at 35,000 rpm for 16 h at 4 °C, and fractions (500 μL each) were collected from the bottom of the tube. The density of each fraction was estimated by weighing a 100-μL drop from fractions of a gradient run.

Partially purified HCV was prepared by collecting the peaks of HCV-core and HCV-RNA and was used for the infection assay and for characterization.

2.10. Quantification of HCV-core protein and RNA

To estimate the levels of HCV-core proteins, the concentration of HCV-core proteins was measured. Aliquots of samples were

assayed using the HCV Core ELISA kit (Ortho Clinical Diagnostics, Tokyo, Japan). Viral RNA was isolated from harvested culture media or from sucrose density gradient fractions using the QiaAmp Viral RNA Extraction kit (Qiagen, Tokyo, Japan). Copy numbers of HCV-RNA were determined by the real-time detection reverse transcription-polymerase chain reaction (RTD-PCR) using an ABI Prism 7500 fast sequence detector system (Applied Biosystems, Tokyo, Japan) [18].

2.11. Immunoprecipitation of HCV particles

Protein G-Sepharose (GE Healthcare, Little Chalfont, UK) was mixed with DMEM-10 for 1 h at 4 °C, and was spun down by centrifugation for 1 min at 5000 rpm (TOMY, Tokyo, Japan). HCV particles (1×10^7 copies HCV-RNA) were mixed with the resin and were incubated overnight at 4 °C with rotation. The sample was centrifuged for 1 min at 5000 rpm, and the supernatant was then collected. A 7.5 μL aliquot of anti-human ApoB (AB742, Millipore, Billerica, MA) or anti-human ApoE polyclonal antibody (AB947, Millipore) was added into the pre-cleared virus fluid (100 μL), and the mixture was incubated overnight at 4 °C. Mouse IgG (5 μg, Sigma) was used as a control. The mixture was mixed with the resin and incubated for 1 h at 4 °C, with rotation. The supernatants were collected following centrifugation and the pellets were then washed twice with PBS and suspended in DMEM-10. Viral RNA was eluted from both the supernatants and the suspended pellets using the QIAamp Viral RNA mini kit (Qiagen). The HCV-RNA titer present in each total RNA from the supernatant and the pellet was evaluated, and the infectivity of the supernatant was measured by inoculation of naïve Huh7.5.1 cells.

3. Results

3.1. Establishment of serum-free cultured Huh7 cells

Huh7 cells are routinely maintained in our laboratory by culture in 10% FCS-supplemented medium. To examine HCV particles produced from infected cells cultured under serum-free conditions, we first established a serum-free culture system which allowed the proliferation of Huh7 cells. It was previously reported that Huh7 cells could be cultured in serum-free media that contains selenium [6]. We therefore examined the growth of Huh7 cells following gradual reduction of the level of FBS and ultimately culture in completely serum-free, selenium-supplemented (ITS-containing) media. The cells could be passaged and cultured over a long period in this medium, although the observed growth, as assayed using an MTS assay, was slightly lower than that of FBS-supplemented cultures for all the cell lines used in this study (Fig. 1 and Supplementary Fig. S1). Based on this result, we used ITS-supplemented media for the evaluation of serum-free cultured HCV.

3.2. Production of HCV particles from serum-free cultures

We next tested the efficiency of HCV particle production in serum-free culture. *In vitro* transcribed HCV-RNAs were transfected into the CD81-negative Huh7-25, and the CD81 positive Huh7-25-CD81 cell lines. The re-infection rate is known to be negligible when Huh7-25 is used [19]. When synthetic RNAs of JFH-1 or J6/JFH-1 strains were transfected, the HCV-core protein and HCV-RNA were detected in the culture media, and each medium was infectious for naïve Huh7 cells (Fig. 2, Supplementary Table). The specific infectivity of each medium (the values of the infectivity titer divided by the values of the HCV-core protein or of HCV-RNA) of J6/JFH-1 HCV was higher than that of JFH-1 (Fig. 2C, Supplementary Table). These results showed that infectious HCV was secreted into the culture medium of both cell lines. The slightly higher HCV production of Huh7-25-CD81 cells may be due to re-infection of secreted virus particles. To determine if HCV-infected cells could be cultured for several passages in serum-free medium, serum-free cultured Huh7 cells were inoculated with infectious J6/JFH-1 chimeric HCV at multiplicity of infection (MOI) of 0.2 and were then cultured for a long period, following which the HCV-core protein and HCV-RNA in the culture medium was analyzed. The HCV-core protein and HCV-RNA were continuously detected in serum-free media, and their level was almost equal to that of infected FBS-supplemented Huh7 culture (Fig. 3).

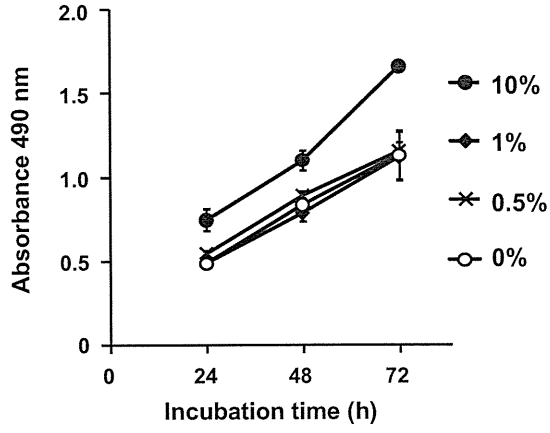

Fig. 1. Cell proliferation assay of serum-free cultured Huh7 cells. Huh7 cells that were seeded into a 96-well plate (1×10^4/well) were sequentially grown in DMEM/F-12 media containing 10%, 1%, 0.5% and 0% fetal bovine serum. At indicated times, an MTS cell proliferation assay was performed using a commercial kit.

3.3. Characterization of serum-free cultured HCV by sucrose density gradient analysis

We next compared the characteristics of HCV viruses produced under serum-free and serum-supplemented conditions by density gradient analysis. Each infectious supernatant was layered on top of a preformed continuous 10–60% sucrose gradient and centrifuged. Eighteen fractions were obtained and HCV-core and RNA titers of each fraction were determined. The detected virus titers in each density fraction were different mainly due to differences in the amount of input virus, as shown in the supplementary table. As previously reported, infectivity of all viruses was observed in fractions of lower density (approximately 1.10 g/mL sucrose) than those in which the peaks of HCV-core and HCV-RNA were detected (Fig. 4), although the specific infectivity of serum-free cultured HCV was slightly lower than that of FBS-supplemented HCV. These results suggested that the infectious HCV produced in the media by serum-free cultures had similar characteristics to those of HCV produced by serum-supplemented cultures. In addition, the virus particles produced from CD81-positive and -negative cells exhibited similar density profiles (Compare Fig. 4A, B vs. C, D).

3.4. Antibodies differentially inhibit HCV from serum-free and serum supplemented cultures

We next examined antibody inhibition of cell infection by HCV derived from serum-free or serum-supplemented cultures. CD81 and SR-BI are candidate cellular receptors for HCV infection. We first determined the inhibitory effect of anti-CD81 and anti-SR-BI antibodies on infection of serum-free cultured HCV. Interestingly, HCV infection by HCV derived from serum-free and serum-supplemented cultures was differently inhibited by these

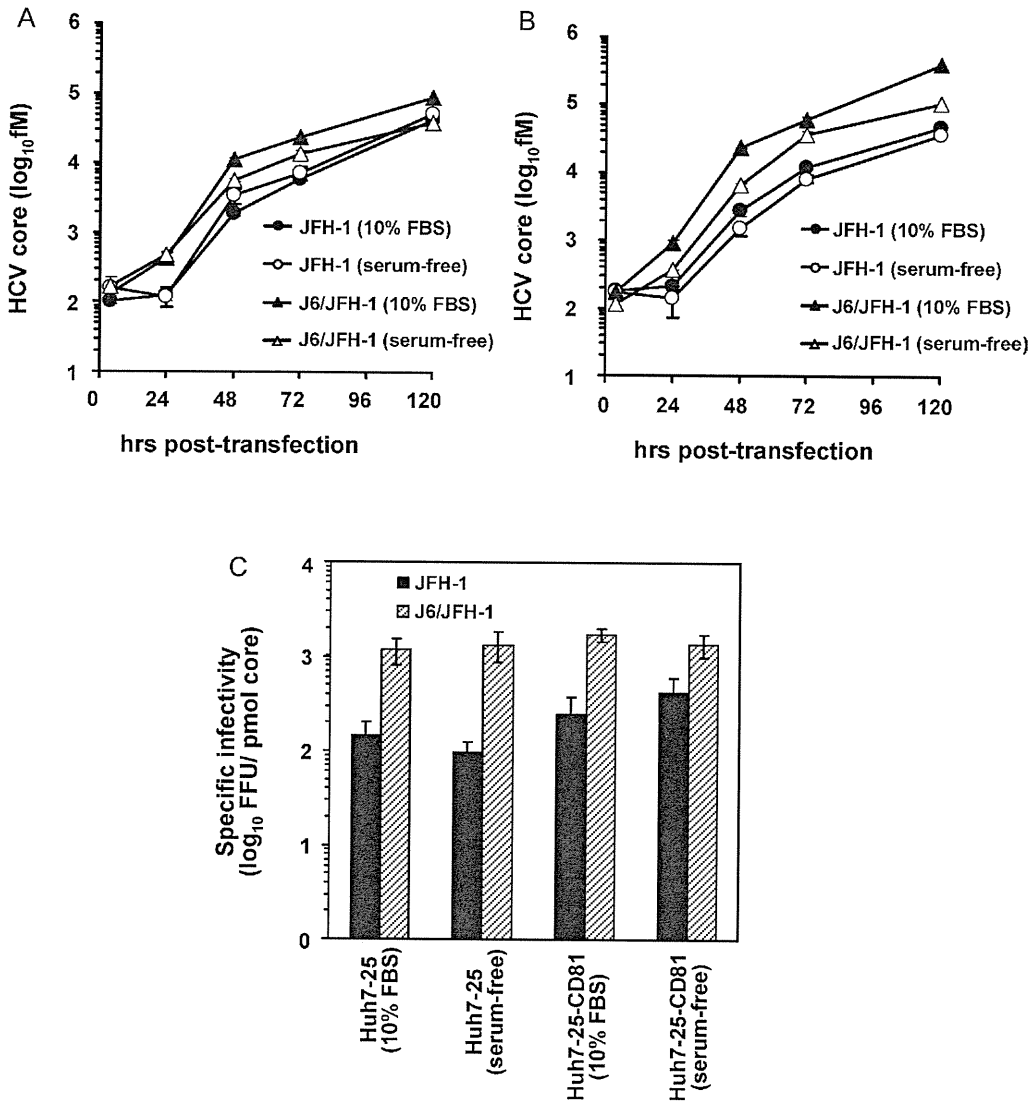

Fig. 2. HCV production from serum-free cultured Huh7 cells transfected with *in vitro* transcribed JFH-1 and J6/JFH-1 RNA. *In vitro* transcribed JFH-1 and J6/JFH-1 RNA was transfected into Huh7-25 (A) and Huh7-25-CD81 (B) cells that were grown under the indicated serum conditions. The culture supernatant was collected 4, 24, 48, 72 and 120 h post-transfection, and the HCV-core protein levels were analyzed using ELISA. All data were measured in triplicate, and are shown as means ± SD. Infectivity of each supernatant that was collected 120 h post-transfection was analyzed by infectivity titration, and specific infectivity was calculated by dividing the mean value of the infectivity titer by that of the HCV-core protein (C). All data were measured in triplicate, and are shown as means ± SD. Profiles of HCV-core, HCV-RNA and infectivity are indicated in the Supplementary Table.

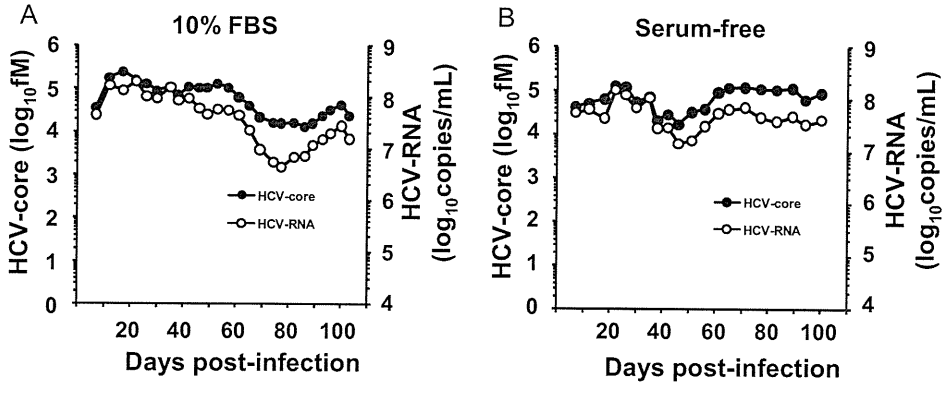

Fig. 3. HCV production from serum-free cultured Huh7 cells infected with J6/JFH-1 HCV. Huh7 cells that were grown in 10% FBS-supplemented (A) or serum-free (B) DMEM/F-12 were inoculated with the J6/JFH-1 virus (MOI, 0.2), and media of sub-cultures were collected. The HCV-core (closed circles) and RNA (open circles) were analyzed using ELISA and RTD-PCR, respectively.

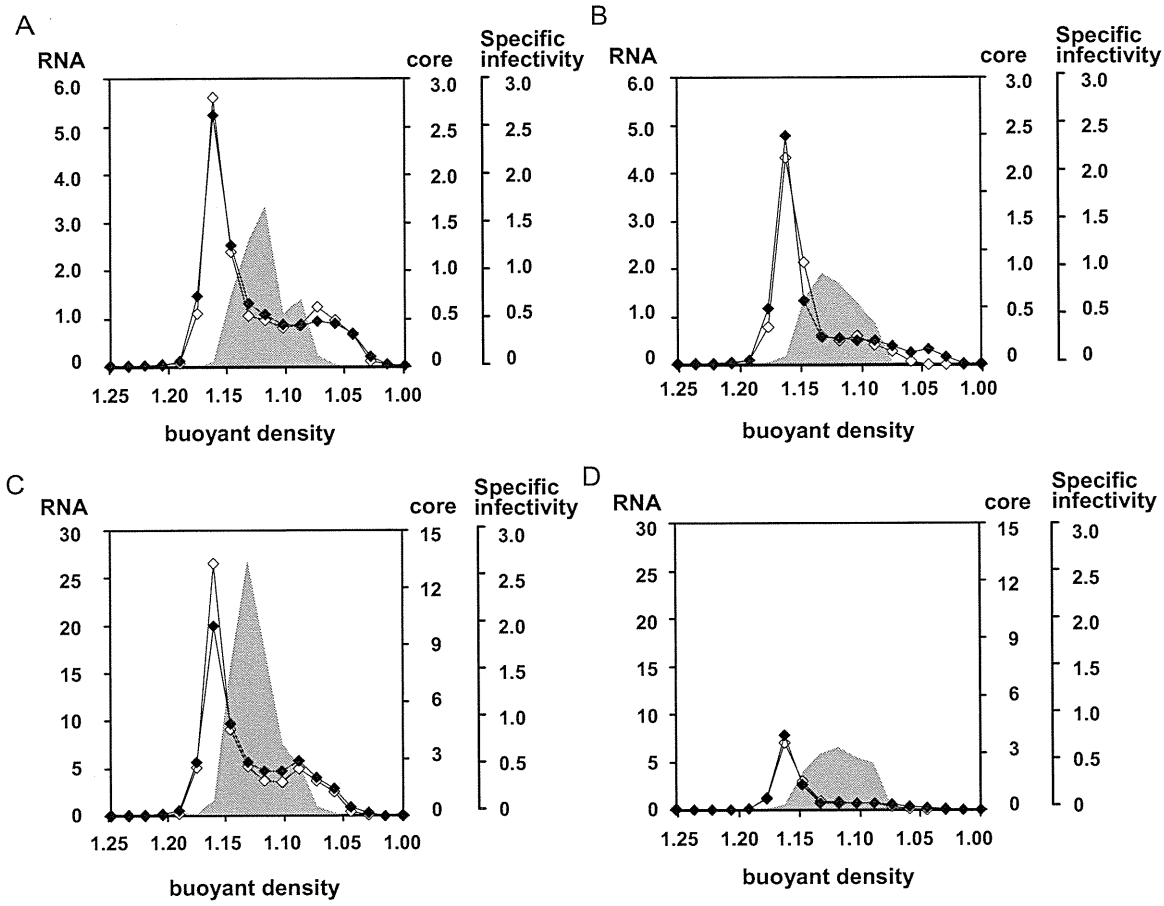

Fig. 4. Density gradient analysis of the supernatants derived from infected serum-free cultured Huh7 cells. *In vitro* transcribed J6/JFH-1 RNA was transfected into Huh7-25 (A and B) and Huh7-25-CD81 (C and D) cells that were cultured under 10% FBS-supplemented (A and C) or serum-free (B and D) conditions. Culture supernatants (4 mL) were collected 5 days post-transfection, and were then layered on top of a preformed continuous 10–60% sucrose gradient in TNE buffer. The gradients were centrifuged using an SW41 rotor at 35,000 rpm for 16 h at 4 °C, and fractions (500 μL each) were collected from the bottom of the tube. The buoyant density (g/mL, *x*-axis), the levels of HCV-core ($\times 10^2$ pM, closed diamonds) and HCV-RNA ($\times 10^8$ copies/mL, open diamonds), and the specific infectivity for naïve Huh7.5.1 cells (FFU/pmol core, shown in gray) of each fraction were analyzed as described in Section 2.

antibodies (Fig. 5A and B). Next, to confirm that the anti-E2 antibody, which has been shown to bind HCV particles, inhibits HCV infection, HCV was pre-incubated with the anti-E2 antibody AP33 and inoculated into Huh7 cells. As shown in previous reports [20,21], AP33 inhibited HCV infection. However, its inhibitory effect was different for serum-free and serum-supplemented cultured HCV. Thus, infection of serum-free cultured HCV displayed the highest susceptibility to this antibody (Fig. 5C).

It has also been recently reported that VLDL associates with HCV and affects infectious particle formation and infection [7–9,22,23]. We therefore determined whether apolipoproteins associate with serum-free cultured HCV by immunoprecipitation of apolipoproteins from the culture media with anti-human apolipoprotein antibodies, followed by analysis of the viral titer in the pellet and the supernatant. HCV particles from both serum-free and serum-supplemented cultures were associated with both ApoB and ApoE (Fig. 6A). The percent of HCV from FBS-supplemented and serum-free cultures respectively that was associated with ApoB was $13.22 \pm 0.09\%$ and $16.84 \pm 0.08\%$ ($p < 0.05$, *t*-test) and the percent associated with ApoE was $20.77 \pm 0.33\%$ and $10.04 \pm 0.04\%$ ($p < 0.005$, *t*-test). Thus, serum-free HCV particles had a larger amount of associated ApoB, and a smaller amount of ApoE, than HCV from serum-supplemented cultures. We next determined whether depletion of ApoE affects viral infectivity by measurement of the infectivity titers of the virus in the supernatant following ApoE precipitation. This experiment showed that the infectivity of HCV from FBS-supplemented cultures, but not of HCV from serum-free cultures, was down-regulated by depletion of ApoB and ApoE (Fig. 6C). These results indicated that apolipoprotein associates differently with viral particles derived from FBS-supplemented and serum-free cultures, and, further, that the infectivity of HCV derived from serum-free culture is only weakly affected by the associated apolipoprotein. These data therefore suggest that, unlike HCV from serum supplemented culture, and in contrast to previous reports regarding HCV infection, infection of HCV derived from serum-free culture may be apolipoprotein-independent. However, further studies are required to confirm this possibility.

4. Discussion

In this study, we established a serum free cell culture system for the production of HCV particles, and compared the characteristics of these particles to those of HCV particles derived from serum-supplemented cultures. The particles derived from serum-free culture were infectious, suggesting that these particles would provide an appropriate antigen for the development of antibodies and vaccines. The serum-free cultured HCV could infect naïve Huh7 cells. Furthermore, sucrose density gradient analysis indicated that the profiles of HCV-core protein and HCV-RNA of serum-free cultured HCV were almost the same as those of HCV from FBS-supplemented cultures. Under serum-free conditions, HCV components (core protein and RNA) tended to be

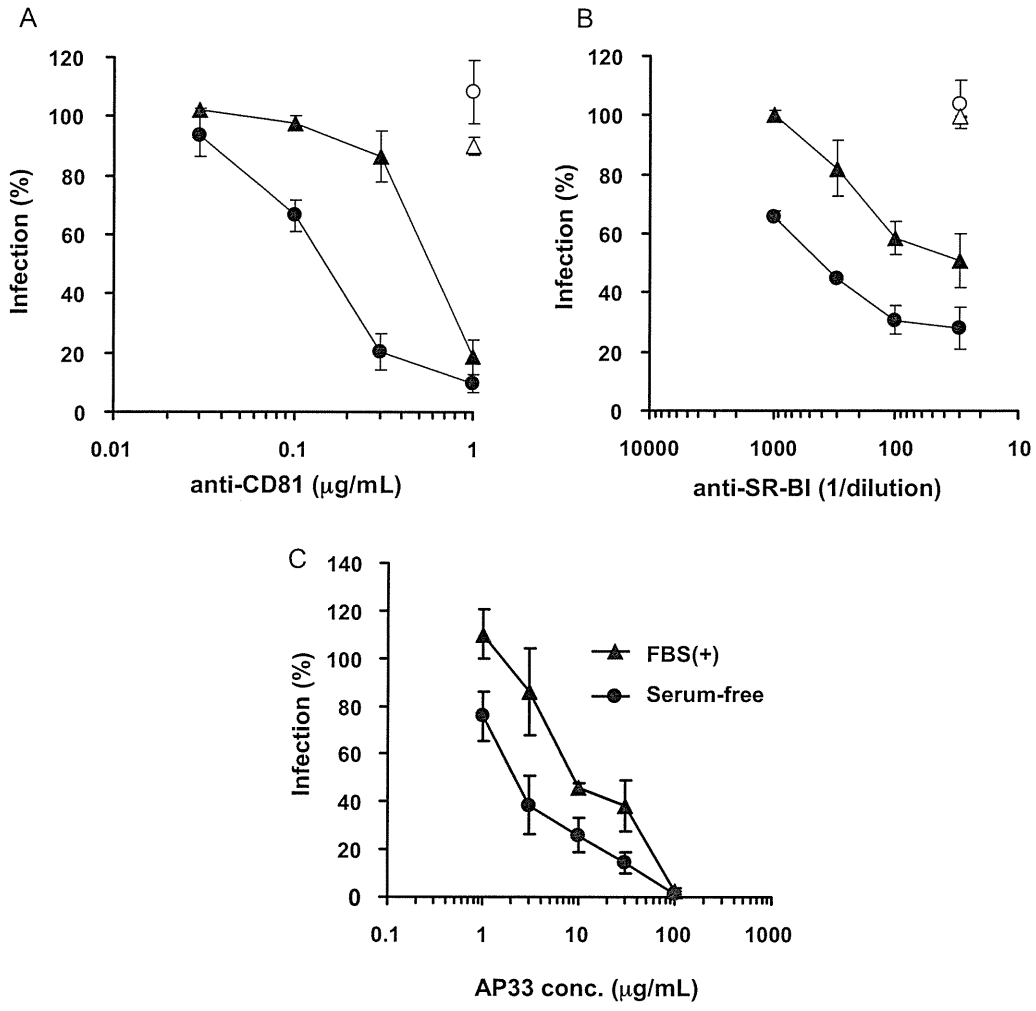

Fig. 5. Inhibition of serum-free cultured HCV infection by anti-CD81, anti-SR-BI and anti-E2 antibodies. Huh7.5.1 cells were pre-incubated with serially diluted anti-CD81 (JS-81, panel A) or anti-SR-BI (panel B) antibody for 1 h, and infectious J6/JFH-1 virus (MOI 0.1) obtained from FBS-supplemented (triangles) or serum-free (circles) culture was inoculated into each well for 72 h. Cells were lysed and HCV-core protein was measured. As controls, 1 μg/mL of mouse IgG (open triangles) and 30-fold diluted rat serum (open circles) were used. For incubation of virus particles with antibody, infectious J6/JFH-1 virus obtained from FBS-supplemented (closed triangle) or serum-free (closed circle) cultures was mixed with the indicated concentration of anti-E2 (AP33, panel C) antibody, and was then inoculated into naïve Huh7.5.1 cells. Infectivity was calculated by titration.

lost from fractions of lower density. Since exosome-like multivesicular particles have been reported to be present in lower density fractions [10], production of multivesicular particles may be different between serum-free and serum-supplemented cultures. When culture supernatants were used, the specific infectivity of serum-free cultured HCV was almost identical to that of FBS-supplemented HCV. However, infectivity of fractions separated on sucrose density gradients was lower for serum-free cultured HCV than for FBS-supplemented HCV cultures. These data may indicate that host factors that contribute to HCV infection differed under different culture conditions. Following infection and subsequent long-term culture under either serum-free or serum-supplemented conditions, HCV-core and RNA levels were identical for the first 40 days, but after this time period the ratio of HCV-core protein:RNA increased in both cultures. This result suggested that long-term culture may induce HCV-core protein which did not have HCV-RNA. As shown in Fig. 3, virus production under serum-free conditions seems to be more stable over 100 days than production under 10% FBS conditions. Fluctuation of viral titer during continuous cultivation of HCV-infected cells has been previously reported [24]. This fluctuation is dependent on the appearance of non-permissive cells with low or no CD81 expression. It is thus likely that these non-permissive cells appear more rapidly under 10% FBS culture conditions than under serum-free conditions. This result may be due to the higher cellular growth rate of these cells in serum-supplemented culture as shown in Fig. 1 and Supplementary Fig. S1.

Our study highlighted some differences between HCV that was produced under serum-free and serum-supplemented conditions. Thus, interestingly, serum-free cultured HCV showed a higher susceptibility to antibody inhibition of viral infection than HCV from serum-supplemented cultures. The multiplicity of infection (MOI) of partially purified HCV was calculated and an MOI of 0.02 was used for HCV infection of naïve Huh7 cells. Although infection by HCV produced under both culture conditions was inhibited by anti-CD81, anti-SR-BI and anti-E2 antibodies in a dose-dependent manner, the degree of antibody inhibition at each dose was stronger for serum-free cultured HCV than for HCV from serum-supplemented cultures (Fig. 5). The anti-CD81 and anti-SR-BI antibody targets the host cells, since CD81 and SR-BI are candidate cellular receptors for HCV. In contrast, the anti-E2 antibody AP33 is a neutralizing antibody for HCV [20,21], and targets virus particles. The antibody inhibition result obtained therefore suggested that HCV infection was affected by contaminating pro-

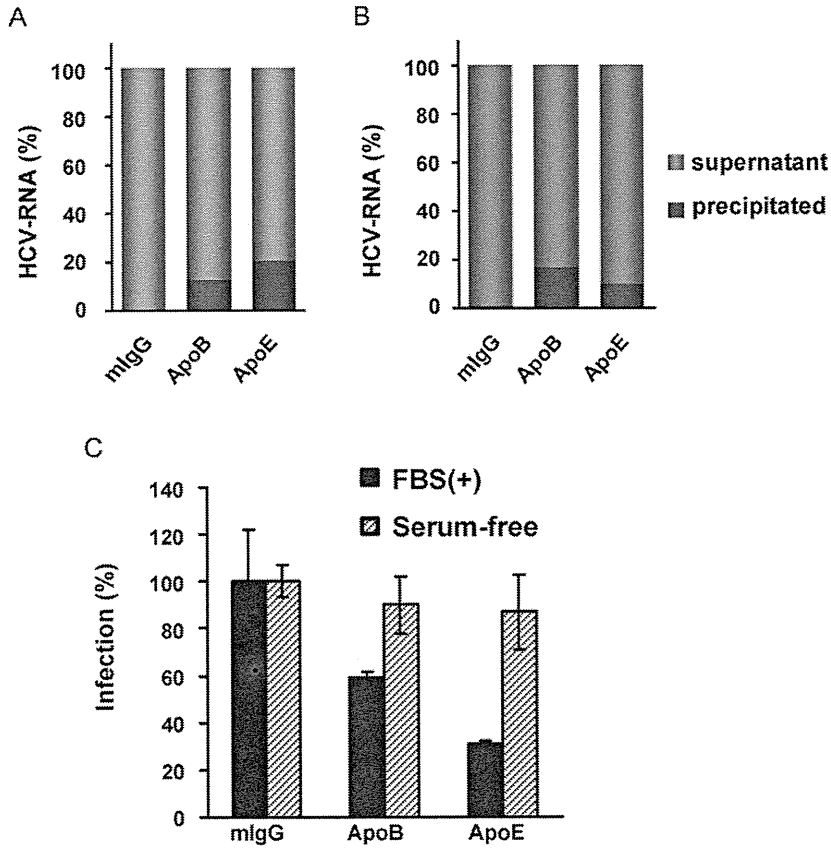

Fig. 6. Immunoprecipitation of cell-cultured HCV with anti-ApoB and ApoE antibodies. 1×10^7 HCV-RNA copies of the J6/JFH-1 virus were incubated with mouse IgG, anti-ApoB or anti-ApoE antibodies, and were then precipitated using protein G-Sepharose. Virus RNA was extracted from the supernatant and the precipitated resin, and HCV-RNA was analyzed using RTD-PCR. All experiments were performed in triplicate, and data are shown as percentages of the mean (A: serum-supplemented, B: serum-free cultured, HCV). Infectivity of the antibody-depleted virus (supernatant) was determined by inoculation into naïve Huh7.5.1 cells. All experiments were performed in triplicate, and data are shown as means ± SD. All data are indicated as percentage of infection, in which the infectivity (FFU/mL) of the supernatant from the mouse IgG (mIgG) precipitation was designated as 100% (C).

teins or by characteristics of HCV that arose due to the different culture conditions used for HCV production. Since CD81-negative Huh7 cells were also able to produce infectious HCV, and since anti-CD81 and anti-E2 antibodies similarly inhibited infection by HCV produced in serum-free culture (data not shown), it is highly unlikely that viral incorporation of CD81 that is produced by CD81-expressing virus-producing cells modulates anti-CD81-inhibition of viral infection. An alternative possibility was that the different antibody inhibition results may have been due to differences in the level, or type of apolipoprotein associated with HCV. HCV associates with lipoproteins in human sera [25], and it has been reported that the envelope proteins of HCV interact with lipoproteins [26]. Moreover, in a recent study, VLDL was reported to associate with HCV particles and affect viral infection and virus secretion [22,23]. Mature VLDL is composed of the apolipoproteins B, C-II and E, as well as lipid, and ApoB and ApoE have been reported to be important for the infectivity of HCV particles [22,23,27–29]. We found that the content of ApoB and ApoE in HCV from serum-supplemented and serum-free cultures was different (Fig. 6A). Thus, serum-free HCV particles had a greater amount of associated ApoB, and a lesser amount of ApoE, than HCV from serum-supplemented cultures. Since ApoE is usually only found in mature VLDL, the serum-free cultured HCV may associate with immature VLDL. A second difference related to associated apolipoprotein of HCV grown under different serum conditions is that the infectivity of HCV from serum-supplied culture, but not that of serum-free cultured HCV, was down-regulated by antibody depletion of ApoB and ApoE. This result suggested that the infection of HCV from serum-supplemented culture, but not infection of serum-free cultured HCV, depended on apolipoproteins. It is possible that production of HCV in serum-free culture results in the formation of HCV particles that differ in lipid and lipoprotein composition from particles produced under serum-supplemented conditions. Consequently, the affinity of serum-free cultured HCV for its cellular receptor might have been altered, and its susceptibility to antibody inhibition of infectivity may have been increased. However, further analysis of the lipid content of HCV grown under different serum conditions is necessary to confirm this point.

Production of HCV using a serum-free culture system has advantage for vaccine development because there is low protein contamination, it facilitates simple viral purification procedures, and it does not involve the use of animals. Furthermore, lipoproteins associated with virus particles may shield conserved epitopes. Purified virus particles produced under serum-free conditions may have these shielded epitopes exposed and thus potentially become stronger immunogens for the induction of neutralizing antibodies. In this study, serum-free cultured HCV was infectious *in vitro*, and the viral particles had a form similar to that of native enveloped viruses. However, we have not yet confirmed the antigenic or immunogenetic properties of serum-free cultured HCV, which would be important for its potential use as a vaccine. Nevertheless, we have recently designed a system for the purification of HCV particles (Morikawa, unpublished data) which will allow testing of these parameters. If these purified particles have high antigenicity, then a HCV vaccine that is derived from HCV produced in cell culture may be available in the future.

5. Conclusions

Infectious HCV could be efficiently produced in serum-free culture. However, the serum-free cultured HCV was highly susceptible to anti-CD81, anti-SR-BI and anti-E2 inhibition of infectivity. The content of ApoB and ApoE in HCV from serum-supplemented and serum-free cultures was different and the infectivity of serum-free cultured HCV appeared to be independent of apolipoproteins. Therefore, lipids conjugated with HCV may affect virus infection and neutralization.

Acknowledgements

This work was partially supported by a grant-in-aid for Scientific Research from the Japan Society for the Promotion of Science and from the Ministry of Health, Labor, and Welfare of Japan by the Research on Health Sciences Focusing on Drug Innovation from the Japan Health Sciences Foundation. Huh7.5.1 was a kind gift from Dr. Francis V. Chisari. Anti-SR-BI antibody and rat serum were kind gifts from Dr. H. Barth. Antibody AP33 was a kind gift from Genentech, Inc.

Appendix A. Supplementary data

Supplementary data associated with this article can be found, in the online version, at doi:10.1016/j.vaccine.2011.04.069.

References

[1] Kato T, Date T, Miyamoto M, Furusaka A, Tokushige K, Mizokami M, et al. Efficient replication of the genotype 2a hepatitis C virus subgenomic replicon. Gastroenterology 2003;125:1808–17.
[2] Wakita T, Pietschmann T, Kato T, Date T, Miyamoto M, Zhao Z, et al. Production of infectious hepatitis C virus in tissue culture from a cloned viral genome. Nat Med 2005;11:791–6.
[3] Lindenbach BD, Evans MJ, Syder AJ, Wolk B, Tellinghuisen TL, Liu CC, et al. Complete replication of hepatitis C virus in cell culture. Science 2005;309:623–6.
[4] Zhong J, Gastaminza P, Cheng G, Kapadia S, Kato T, Burton DR, et al. Robust hepatitis C virus infection in vitro. Proc Natl Acad Sci USA 2005;102:9294–9.
[5] Gottwein JM, Scheel TK, Jensen TB, Lademann JB, Prentoe JC, Knudsen ML, et al. Development and characterization of hepatitis C virus genotype 1–7 cell culture systems: role of CD81 and scavenger receptor class B type I and effect of antiviral drugs. Hepatology 2009;49:364–77.
[6] Nakabayashi H, Taketa K, Miyano K, Yamane T, Sato J. Growth of human hepatoma cells lines with differentiated functions in chemically defined medium. Cancer Res 1982;42:3858–63.
[7] Andre P, Komurian-Pradel F, Deforges S, Perret M, Berland JL, Sodoyer M, et al. Characterization of low- and very-low-density hepatitis C virus RNA-containing particles. J Virol 2002;76:6919–28.
[8] Nielsen SU, Bassendine MF, Burt AD, Martin C, Pumeechockchai W, Toms GL. Association between hepatitis C virus and very-low-density lipoprotein (VLDL)/LDL analyzed in iodixanol density gradients. J Virol 2006;80:2418–28.
[9] Nielsen SU, Bassendine MF, Martin C, Lowther D, Purcell PJ, King BJ, et al. Characterization of hepatitis C RNA-containing particles from human liver by density and size. J Gen Virol 2008;89:2507–17.
[10] Gastaminza P, Dryden K, Boyd B, Wood M, Law M, Yeager M, et al. Ultrastructural and biophysical characterization of hepatitis C virus particles produced in cell culture. J Virol 2010;84:10999–1009.
[11] Masciopinto F, Giovani C, Campagnoli S, Galli-Stampino L, Colombatto P, Brunetto M, et al. Association of hepatitis C virus envelope proteins with exosomes. Eur J Immunol 2004;34:2834–42.
[12] Akazawa D, Date T, Morikawa K, Murayama A, Miyamoto M, Kaga M, et al. CD81 expression is important for the permissiveness of Huh7 cell clones for heterogeneous hepatitis C virus infection. J Virol 2007;81:5036–45.
[13] Murayama A, Date T, Morikawa K, Akazawa D, Miyamoto M, Kaga M, et al. The NS3 helicase and NS5B-to-3′X regions are important for efficient hepatitis C virus strain JFH-1 replication in Huh7 cells. J Virol 2007;81:8030–40.
[14] Kato T, Date T, Murayama A, Morikawa K, Akazawa D, Wakita T. Cell culture and infection system for hepatitis C virus. Nat Protoc 2006;1:2334–9.
[15] Date T, Miyamoto M, Kato T, Morikawa K, Murayama A, Akazawa D, et al. An infectious and selectable full-length replicon system with hepatitis C virus JFH-1 strain. Hepatol Res 2007;37:433–43.
[16] Barth H, Cerino R, Arcuri M, Hoffmann M, Schürmann P, Adah MI, et al. Scavenger receptor class B type I and hepatitis C virus infection of primary Tupaia hepatocytes. J Virol 2005;79:5774–85.
[17] Murakami K, Kimura T, Osaki M, Ishii K, Miyamura T, Suzuki T, et al. Virological characterization of the hepatitis C virus JFH-1 strain in lymphocytic cell lines. J Gen Virol 2008;89:1587–92.
[18] Takeuchi T, Katsume A, Tanaka T, Abe A, Inoue K, Tsukiyama-Kohara K, et al. Real-time detection system for quantification of hepatitis C virus genome. Gastroenterology 1999;116:636–42.
[19] Kato T, Choi Y, Elmowalid G, Sapp RK, Barth H, Furusaka A, et al. Hepatitis C virus JFH-1 strain infection in chimpanzees is associated with low pathogenicity and emergence of an adaptive mutation. Hepatology 2008;48:732–40.
[20] Owsianka A, Tarr AW, Juttla VS, Lavillette D, Bartosch B, Cosset FL, et al. Monoclonal antibody AP33 defines a broadly neutralizing epitope on the hepatitis C virus E2 envelope glycoprotein. J Virol 2005;79:11095–104.
[21] Tarr AW, Owsianka AM, Timms JM, McClure CP, Brown RJ, Hickling TP, et al. Characterization of the hepatitis C virus E2 epitope defined by the broadly neutralizing monoclonal antibody AP33. Hepatology 2006;43:592–601.
[22] Gastaminza P, Cheng G, Wieland S, Zhong J, Liao W, Chisari FV. Cellular determinants of hepatitis C virus assembly, maturation, degradation, and secretion. J Virol 2008;82:2120–9.
[23] Huang H, Sun F, Owen DM, Li W, Chen Y, Gale Jr M, et al. Hepatitis C virus production by human hepatocytes dependent on assembly and secretion of very low-density lipoproteins. Proc Natl Acad Sci USA 2007;104:5848–53.
[24] Zhong J, Gastaminza P, Chung J, Stamataki Z, Isogawa M, Cheng G, et al. Persistent hepatitis C virus infection in vitro: coevolution of virus and host. J Virol 2006;80:11082–93.
[25] Thomssen R, Bonk S, Propfe C, Heermann KH, Kochel HG, Uy A. Association of hepatitis C virus in human sera with beta-lipoprotein. Med Microbiol Immunol 1992;181:293–300.
[26] Monazahian M, Kippenberger S, Muller A, Seitz H, Bohme I, Grethe S, et al. Binding of human lipoproteins (low, very low, high density lipoproteins) to recombinant envelope proteins of hepatitis C virus. Med Microbiol Immunol 2000;188:177–84.
[27] Benga WJ, Krieger SE, Dimitrova M, Zeisel MB, Parnot M, Lupberger J, et al. Apolipoprotein E interacts with hepatitis C virus nonstructural protein 5A and determines assembly of infectious particles. Hepatology 2010;51:43–53.
[28] Chang KS, Jiang J, Cai Z, Luo G. Human apolipoprotein E is required for infectivity and production of hepatitis C virus in cell culture. J Virol 2007;81:13783–93.
[29] Jiang J, Luo G. Apolipoprotein E but not B is required for the formation of infectious hepatitis C virus particles. J Virol 2009;83:12680–91.

GASTROENTEROLOGY 2011;141:128–140

Malnutrition Impairs Interferon Signaling Through mTOR and FoxO Pathways in Patients With Chronic Hepatitis C

MASAO HONDA,*,‡ KENJI TAKEHANA,§ AKITO SAKAI,* YUSUKE TAGATA,§ TAKAYOSHI SHIRASAKI,‡ SHINOBU NISHITANI,§ TAKAHIKO MURAMATSU,‖ TATSUYA YAMASHITA,* YASUNARI NAKAMOTO,* EISHIRO MIZUKOSHI,* YOSHIO SAKAI,* TARO YAMASHITA,* MIKIKO NAKAMURA,* TETSURO SHIMAKAMI,¶ MINKYUNG YI,# STANLEY M. LEMON,¶ TETSUO SUZUKI,** TAKAJI WAKITA,** SHUICHI KANEKO,* and the Hokuriku Liver Study Group

*Department of Gastroenterology, ‡Department of Advanced Medical Technology, Kanazawa University Graduate School of Medicine, Kanazawa, Japan; §Exploratory Research Laboratories, Research Center, Ajinomoto Pharmaceuticals, Co, Ltd, Kanagawa, Japan; ‖Frontier Research Labs, Institute for Innovation, Ajinomoto, Co, Inc, Kanagawa, Japan; ¶Division of Infectious Diseases, School of Medicine, The University of North Carolina at Chapel Hill, Chapel Hill, North Carolina; #Center for Hepatitis Research, Institute for Human Infections and Immunity, and Department of Microbiology and Immunology, University of Texas Medical Branch, Galveston, Texas; and **Department of Virology II, National Institute of Infectious Diseases, Tokyo, Japan

BACKGROUND & AIMS: Patients with advanced chronic hepatitis C (CH-C) often are malnourished, but the effects of malnutrition on interferon (IFN) signaling and response to treatment have not been determined. We assessed the importance of the nutritional state of the liver on IFN signaling and treatment response. **METHODS:** We studied data from 168 patients with CH-C who were treated with the combination of pegylated-IFN and ribavirin. Plasma concentrations of amino acids were measured by mass spectrometry. Liver gene expression profiles were obtained from 91 patients. Huh-7 cells were used to evaluate the IFN signaling pathway, mammalian target of rapamycin complex 1 (mTORC1), and forkhead box O (FoxO). Antiviral signaling induced by branched-chain amino acids (BCAAs) was determined using the in vitro hepatitis C virus replication system. **RESULTS:** Multivariate logistic regression analysis showed that Fischer's ratio was associated significantly with nonresponders, independent of interleukin-28B polymorphisms or the histologic stage of the liver. Fischer's ratio was correlated inversely with the expression of BCAA transaminase 1, and was affected by hepatic mTORC1 signaling. IFN stimulation was impaired substantially in Huh-7 cells grown in medium that was low in amino acid concentration, through repressed mTORC1 signaling, and increased Socs3 expression, which was regulated by Foxo3a. BCAA could restore impaired IFN signaling and inhibit hepatitis C virus replication under conditions of malnutrition. **CONCLUSIONS: Malnutrition impaired IFN signaling by inhibiting mTORC1 and activating Socs3 signaling through Foxo3a. Increasing BCAAs to up-regulate IFN signaling might be used as a new therapeutic approach for patients with advanced CH-C.**

Keywords: HCV; Liver Disease; Therapy; Diet.

Interferon (IFN) and ribavirin (RBV) combination therapy is a popular modality for treating patients with chronic hepatitis C (CH-C), but approximately 50% of patients usually relapse, particularly those with hepatitis C virus (HCV) genotype 1b and a high viral load.[1]

Recent landmark studies of genome-wide associations identified genomic loci associated with treatment responses to pegylated (Peg)-IFN and RBV combination therapy,[2,3] and a polymorphism in the interleukin (IL)-28B gene was found to predict hepatitis C treatment-induced viral clearance. Moreover, we previously showed that expression of hepatic IFN-stimulated genes (ISGs) was associated with the IL-28B polymorphism and might contribute to the treatment response.[4] In addition to the IL-28B polymorphism, host factors such as fibrosis stage and metabolic status of the liver might be associated with the treatment outcome[4,5]; however, the significance of these factors in conjunction with the IL-28B polymorphism has not been evaluated fully.

In CH-C livers, prolonged liver cell damage, fibrosis development, and microcirculation failure can lead to a state of malnutrition in hepatocytes, resulting in the impairment of multiple metabolic pathways. In patients with advanced stage CH-C, hypoalbuminemia and decreased plasma values for the Fischer's ratio of branched-amino acids (BCAA; leucine, isoleucine, and valine) to aromatic amino acids (tyrosine and phenylalanine) commonly are observed. BCAA are the essential amino acids necessary for ammonium metabolism in muscle when the liver is unable to perform this function. Recent reports have shown that BCAA activates albumin synthesis in rat

Abbreviations used in this paper: BCAA, branched-chain amino acid; BCAT1, branched chain amino-acid transaminase 1; CH-C, chronic hepatitis C; ChIP, chromatin immunoprecipitation; DMEM, Dulbecco's modified Eagle medium; FBE, Foxo binding element; FBEmut, Foxo binding element mutant; FoxO, forkhead box, subgroup O; GLuc, Gaussia luciferase; IFN, interferon; IL, interleukin; ISG, interferon-stimulated genes; mTOR, mammalian target of rapamycin; mTORC1, mammalian target of rapamycin complex 1; NR, no response; PCR, polymerase chain reaction; Peg, pegylated; p-mTOR, phosphorylated form of mammalian target of rapamycin; pS6K, phosphorylated form of p70 S6 protein kinase; pSTAT1, phosphorylated form of signal transducer and activator of transcription 1; Raptor, regulatory associated protein of mTOR; RBV, ribavirin; S6K, p70 S6 protein kinase; siRNA, small interfering RNA; SVR, sustained viral response; TR, transient response.

0016-5085/$36.00
doi:10.1053/j.gastro.2011.03.051

primary hepatocytes[6] and cirrhotic rat liver[7] through mammalian target of rapamycin (mTOR) signaling, a central regulator of protein synthesis, by sensing nutrient conditions.[8] Thus, peripheral amino acid composition is closely related to signaling pathways in the liver.

In addition to metabolic aspects, recent reports have elucidated new functional roles for mTOR in the IFN signaling pathway. Targeted disruptions of tuberous sclerosis 2 and eukaryotic translation initiation factor 4E binding protein 1, which both inhibit mTOR complex 1 (mTORC1) signaling, substantially enhanced IFN-alfa–dependent antiviral responses.[9,10] Therefore, mTORC1 signaling might be involved in the antiviral response as well as in metabolic processes. However, these issues have not yet been addressed in terms of IFN treatment for CH-C. In the present study, therefore, we evaluated the clinical relevance of the nutritional state of the liver, as estimated by the plasma Fischer's ratio, on Peg-IFN and RBV combination therapy. We also evaluated antiviral signaling induced by BCAA using an in vitro HCV replication system.

Materials and Methods

Patients

A total of 168 patients with CH-C at the Graduate School of Medicine at Kanazawa University Hospital (Kanazawa, Japan) and its related hospitals in Japan (Table 1, Supplementary Table 1) were evaluated in the present study. The clinical characteristics of these patients have been described previously.[4] All patients were administered Peg–IFN-alfa 2b (Schering-Plough K.K., Tokyo, Japan) and RBV combination therapy for 48 weeks. The definition of the treatment response was as follows: sustained viral response (SVR), clearance of HCV viremia 24 weeks after the cessation of therapy; transient response (TR), no detectable HCV viremia at the cessation of therapy but relapse during the follow-up period; and no response (NR). Genetic variation of the IL-28B polymorphism at rs8099917 was evaluated in all patients using TaqMan Pre-Designed SNP Genotyping Assays (Applied Biosystems, Carlsbad, CA) as described previously.[4] Gene expression profiling in the liver was performed in 91 patients using the Affymetrix Human 133 Plus 2.0 microarray chip (Affymetrix, Santa Clara, CA) as described previously (Supplementary Table 1).[4]

Plasma Amino Acid Analysis

Amino acid concentrations in plasma samples were measured by high-performance liquid chromatography–electrospray ionization–mass spectrometry, followed by derivatization.[11] Detailed experimental procedures are described in the Supplementary Materials and Methods section.

Culture Medium

Huh-7 and Huh-7.5 cells (kindly provided by Professor C. M. Rice, Rockefeller University, New York, NY) were maintained in Dulbecco's modified Eagle medium (DMEM; Gibco BRL, Gaithersburg, MD) containing 10% fetal bovine serum and 1% penicillin/streptomycin (normal medium). Amino acid-free medium (ZERO medium) was prepared by mixing 5.81 g nutrition-free DMEM (Nacalai Tesque, Kyoto, Japan), 1.85 g $NaHCO_3$, 1 g glucose, and 0.5 mL 1M (mol/L) sodium pyruvate in 500 mL Milli-Q water, then sterilizing with a 0.22-μm filter (Millipore, Billerica, MA). Low amino acid media ($\times$1/5, $\times$1/10, $\times$1/30, and $\times$1/100 DMEM) were prepared by diluting $\times$1 DMEM with ZERO medium. Powdered BCAA (leucine-isoleucine-valine, 2:1:1.2) (Ajinomoto Pharma, Tokyo, Japan) was freshly dissolved with distilled water at 100 mmol/L, then applied to cultured medium at 2 mmol/L, 4 mmol/L, or 8 mmol/L.

Western Blotting and Immunofluorescence Staining

A total of 1.5×10^5 Huh-7 cells were seeded in normal medium 24 hours before performing the experiments. The medium was changed to low-amino-acid medium and maintained for up to 24 hours. Western blotting was performed as previously described.[12] Cells were washed in phosphate-buffered saline (PBS) and lysed in RIPA buffer containing complete Protease Inhibitor Cocktail and PhosSTOP (Roche Applied Science, Indianapolis, IN). The membranes were blocked in Blocking One-P (Nacalai Tesque). The antibodies used for Western blotting are summarized in the Supplementary Materials and Methods section.

For immunofluorescence staining, cells were fixed with 4% paraformaldehyde in PBS, then permeabilized with 0.1% Triton-X 100 in PBS. The primary anti-forkhead box O (Foxo)3a antibody (Abcam, Cambridge, MA) was used at a final concentration of 2 μg/mL in PBS containing 2% fetal bovine serum at 4°C for 16 hours. Incubation with the Alexa Fluor 488–conjugated secondary antibody (Invitrogen, Carlsbad, CA) at a 500-fold dilution in PBS containing 3% fetal bovine serum antibody was performed for 4 hours, and cells were stained with Hoechst 33258 to visualize nuclear DNA (Vector Laboratories, Burlingame, CA).

Quantitative Real-Time Detection Polymerase Chain Reaction

A total of 1.5×10^5 Huh-7 cells were seeded in normal medium 24 hours before performing the experiments. The medium was changed to low-amino-acid medium, to which IFN-alfa and/or BCAA was added, and maintained for 24 hours. Rapamycin treatment (100 nmol/L) was performed for 30 minutes in normal medium before a medium change. RNA was isolated using TriPure isolation reagent (Roche Applied Science), and complementary DNA (cDNA) was synthesized using the High Capacity cDNA reverse transcription kit (Applied Biosystems, Carlsbad, CA). Real-time detection polymerase chain reaction (PCR) was performed using the 7500 Real-Time PCR System (Applied Biosystems) and Power SYBR Green PCR Master Mix (Applied Biosystems) containing specific primers according to the manufacturer's

Table 1. Comparison of Clinical Factors Between Patients With and Without NR

Clinical category	SVR+TR	NR	Univariate *P* value	Multivariate odds (95% CI)	Multivariate *P* value
Patients, n	125	43		—	
Age and sex					
Age, y	57 (30–72)	56 (30–73)	.927	—	
Sex, male vs female	68 vs 57	24 vs 19	.872	—	
Liver histology					
F stage (F1–2 vs F3–4)	95 vs 30	20 vs 23	.001	6.35 (2.02–23.7)	.001
A grade (A0–1 vs A2–3)	68 vs 57	19 vs 24	.248	—	
Host gene factors					
IL-28B (TT vs TG/GG)[a]	109 vs 12	12 vs 31	<.001	19.7 (5.74–82.7)	<.001
ISGs (Mx, IFI44, IFIT1), (<3.5 vs ≥3.5)	103 vs 22	12 vs 31	<.001	5.26 (1.65–17.6)	.005
Metabolic factors					
BMI, kg/m^2	23.2 (16.3–34.7)	23.4 (19.5–40.6)	.439	—	
TG, mg/dL	98 (30–323)	116 (45–276)	.058	—	
T-Chol, mg/dL	167 (90–237)	160 (81–214)	.680	—	
LDL-Chol, mg/dL	82 (36–134)	73 (29–123)	.019	—	
HDL-Chol, mg/dL	42 (20–71)	47 (18–82)	.098	—	
FBS, mg/dL	94 (60–291)	96 (67–196)	.139	—	
Insulin, μU/mL	6.6 (0.7–23.7)	6.8 (2–23.7)	.039	—	
HOMA-IR	1.2 (0.3–11.7)	1.2 (0.4–7.2)	.697	—	
Fischer ratio	2.3 (1.5–3.3)	2.1 (1.5–2.8)	.005	8.91 (1.62–55.6)	.011
Other laboratory parameters					
AST level, IU/L	46 (18–258)	64 (21–283)	.017	—	
ALT level, IU/L	60 (16–376)	82 (18–345)	.052	—	
γ-GTP level, IU/L	36 (4–367)	75 (26–392)	<.001	—	
WBC, /mm^3	4800 (2100–11100)	4800 (2500–8200)	.551	—	
Hb level, g/dL	14 (9.3–16.6)	14.4 (11.2–17.2)	.099	—	
PLT, ×104/mm^3	15.7 (7–39.4)	15.2 (7.6–27.8)	.378	—	
Viral factors					
ISDR mutations ≤1 vs ≥2	80 vs 44	34 vs 9	.070	4.12 (1.25–15.9)	.019
HCV-RNA, KIU/mL	2300 (126–5000)	1930 (140–5000)	.725	—	
Treatment factors					
Total dose administered					
Peg-IFN, μg	3840 (960–7200)	3840 (1920–2880)	.916	—	
RBV, g	202 (134–336)	202 (36–336)	.531	—	
Achieved administration rate					
Peg-IFN, %					
≥80%	84	28	.975	—	
<80%	42	14			
RBV (%)					
≥80%	76	24	.745	—	
<80%	50	18			
Achievement of EVR	101/125 (81%)	0/43 (0%)	<.001	—	

BMI, body mass index; CI, confidence interval; FBS, fasting blood sugar; γ-GTP, gamma-glutamyl transpeptidase; Hb, hemoglobin; HDL-chol, high density lipoprotein cholesterol; LDL-chol, low density lipoprotein cholesterol; PLT, platelets; T-chol, total cholesterol; TG, triglycerides; WBC, leukocytes.

[a]IL-28B SNP at rs8099917.

instructions. The primer sequence for real-time detection PCR is given in the Supplementary Materials and Methods section. HCV RNA was detected as described previously[12] and expression was standardized to that of glyceraldehyde-3-phosphate dehydrogenase.

Reporter Assay

Construction of the interferon stimulated response element (ISRE)-luc reporter plasmid and Socs3-luc or Socs3 (FoxO binding element mutant [FBEmut])-luc reporter plasmids is described in the Supplementary Materials and Methods section.

Huh-7 cells were transfected with the ISRE-luc reporter plasmid 24 hours before IFN-alfa treatment. Cells were treated with IFN-alfa (0 or 100 U/mL) and BCAA (2 mmol/L) in low-amino-acid media. After 24 hours, luciferase activities were measured using the Dual Luciferase assay system (Promega, Madison, WI). For Socs3 promoter activities, Huh-7 cells were transfected with Socs3-luc or Socs3 (FBEmut)-luc reporter plasmids together with the Foxo3a expression plasmid, and luciferase activities were measured after 24 hours. Values were normalized to the luciferase activity of the co-transfected pGL4.75 Renilla luciferase-expressing plasmid (Promega).

Knockdown Experiments

Huh-7 cells were transfected with Ctrl (Stealth RNAi Negative Control Low GC Duplex #2; Invitrogen) or

targets (regulatory associated protein of mTOR [Raptor] and Foxo3a) (Supplementary Materials and Methods) small interfering RNA (siRNA) using Lipofectamine RNAiMAX reagent (Invitrogen) according to the manufacturer's instructions. After 48 hours, cells were cultured in normal or low-amino-acid media for a further 24 hours. The knockdown effect was confirmed by Western blotting.

Chromatin Immunoprecipitation Assay

Detailed experimental procedures are described in the Supplementary Materials and Methods section.

HCV Replication Analysis

pH77S3 is an improved version of pH77S, a plasmid containing the full-length sequence of the genotype 1a H77 strain of HCV with 5 cell culture–adaptive mutations that promote its replication in Huh-7 hepatoma cells.[13] pH77S.3/Gaussia luciferase (GLuc)2A is a related construct in which the GLuc sequence, fused to the 2A autocatalytic protease of foot-and-mouth virus RNA, was inserted in-frame between p7 and NS2[14] (Supplementary Materials and Methods). A signal sequence in GLuc directs its secretion into cell culture media, allowing real-time, dynamic measurements of GLuc expression to be performed without the need for cell lysis.

A 10-μg aliquot of synthetic RNA transcribed from pH77S.3/GLuc2A was used for electroporation. Cells were pulsed at 260 V and 950 μF using the Gene Pulser II apparatus (Bio-Rad Laboratories, Hercules, CA) and plated in fresh normal medium for 12 hours to recover. Cell medium was changed to ×1 DMEM without serum for 8 hours, then changed to low-amino-acid medium containing 0–8 mmol/L BCAA for a further 24 hours. Cells and culture medium were collected and used for GLuc assays, real-time detection PCR, and Western blotting. The number of viable cells was determined by a (3-[4,5-dimethylthiazol-2-yl]-5-[3-carboxymethoxyphenyl]-2-[4-sulfophenyl] -2H-tetrazolium, inner salt) assay (Promega).

Continuously JFH-1–infecting Huh-7 cells were obtained by the infection of Huh-7 cells with JFH-1 cell culture-derived HCV at a multiplicity of infection of 0.01. Cells were maintained in normal medium by passaging every 3–4 days for approximately 6 months. About 20%–30% of the cells consistently were positive for HCV core protein (Supplementary Figure 4). Culture medium of JFH-1–infecting Huh-7 cells was changed to the low-amino-acid medium containing 0–8 mmol/L BCAA for 24 hours. Cells then were collected and used for assays.

Statistical Analysis

Results are expressed as mean ± standard deviation. Significance was tested by 1-way analysis of variance with the Bonferroni method, and differences were considered statistically significant at a P value of less than .05.

Results

Fischer's Ratio as a Predictive Factor for Treatment Response

The clinical characteristics of patients who received Peg-IFN and RBV combination therapy are shown in Table 1 and Supplementary Table 1, and explanations of these characteristics have been described previously.[4] All patients were infected with HCV genotype 1b and had a high viral load (>100 IU/mL). We compared patients with SVR + TR against those with NR, as assessed by the overall plausibility of treatment response groups using Fisher's C statistic as previously described.[4] We included data on the IL-28B polymorphism and plasma amino acid composition (aminogram).

Univariate regression analysis showed that no single amino acid was associated significantly with treatment response; however, using Fischer's ratio, the BCAA (Ile+Leu+Val)/aromatic amino acids (Phe+Tyr) ratio was associated significantly with treatment response (P = .005) (Table 1). Of the 121 patients with IL-28B major type, SVR, TR, and NR were observed in 53%, 37%, and 10%, respectively, and among 33 patients with IL-28B minor type, SVR, TR, and NR were observed in 15%, 17%, and 68%, respectively ($P < .001$) (data not shown). Fischer's ratio of SVR, TR, and NR was 2.35 ± 0.38, 2.30 ± 0.29, and 2.10 ± 0.31, respectively ($P < .015$) (data not shown).

We selected IL-28B polymorphism, hepatic ISG expression, fibrosis stage, HCV RNA, interferon sensitivity determining region mutation, and Fischer's ratio as factors for multivariate analysis. Multivariate analysis revealed that the minor type of IL-28B polymorphism (TG or GG at rs8099917) (odds ratio, 19.7; $P < .001$), advanced fibrosis stage of the liver (F3–4) (odds ratio, 6.35; $P = .001$), high hepatic ISGs (≧3.5) (odds ratio, 5.26; $P = .005$), low Fischer's ratio (continuous range, 1.5–3.3) (unit odds, 8.91; $P = .011$), and presence of ISDR mutation (≦1) (odds ratio, 4.12; $P = .019$) independently contributed to NR (Table 1).

The distribution of the Fischer's ratio according to fibrosis stage is shown in Supplementary Figure 1. The ratio decreased significantly in advanced fibrosis stage (F3–4) compared with early fibrosis stage (F1). No significant association between major or minor type of IL-28B polymorphism and different fibrosis stages of the liver was observed (Supplementary Figure 1*A*). In early fibrosis (F1–2) (Supplementary Figure 1*B*), 90% (80 of 89) of SVR+TR cases had the major type of IL-28B polymorphism, and 94% (16 of 17) of NR cases had the minor type. However, in the advanced fibrosis stage of the liver (F3–4) (Supplementary Figure 1*C*), 85% (23 of 27) of SVR+TR cases had the major type of IL-28B polymorphism and 50% (10 of 20) of NR cases had the minor type. Thus, in advanced fibrosis stages, factors other than the IL-28B polymorphism appear to contribute to NR. Interestingly, the Fischer's ratio was significantly lower in NR patients than SVR+TR pa-

tients in the advanced fibrosis stage of the liver. Therefore, Fischer's ratio could be an important predictor for NR that is independent of IL-28B polymorphism and histologic stage of the liver.

Fischer's Ratio and mTORC1 Signaling in CH-C Livers

Hepatic gene expression in 91 of 168 patients (Supplementary Table 1) was obtained using Affymetrix genechip analysis as described previously.[4] To examine the relationship between the plasma Fischer's ratio and mTORC1 signaling in the liver we evaluated the expression of key regulatory genes related to mTORC1 signaling. We found that expression of branched chain amino-acid transaminase 1 (BCAT1), an important catalytic enzyme of BCAA, was significantly negatively correlated with Fischer's ratio (Figure 1*A*). This indicates that the plasma Fischer's ratio is regulated in the liver as well as in peripheral muscle. Interestingly, the expression of c-myc, a positive regulator of BCAT1 (Figure 1*C*),[15] was correlated negatively with the Fischer's ratio (Figure 1*B*). The expression of PDCD4, a negative transcriptional target of ribosomal p70 S6 protein kinase (S6K), downstream of mTORC1, was correlated significantly with BCAT1 (Figure 1*D* and *E*). Thus, in CH-C livers, BCAT1 is induced with progressive liver disease and mTORC1 signaling is repressed, a process that might involve c-myc. Fischer's ratio of the plasma therefore can be seen to reflect mTORC1 signaling in the liver.

Impaired IFN Signaling in Huh-7 Cells Grown in Low-Amino-Acid Medium

Recent reports have shown the functional relevance of mTOR on IFN signaling and antiviral responses.[9,10] To evaluate IFN-alfa signaling and the mTOR pathway, we used Huh-7 cells grown in different amino acid conditions (×1 DMEM, ×1/5 DMEM, ×1/30 DMEM, and ×1/100 DMEM). The phosphorylated forms of mTOR (p-mTOR) and S6K (pS6K), an important downstream regulator of mTORC1 signaling, were decreased substantially in ×1/30 DMEM and ×1/100 DMEM (Figure 2*A*). Interestingly, the expression of the phosphorylated form of signal transducer and activator of transcription 1 (pSTAT1), an essential transducer of type 1 IFN signaling, also was decreased in these conditions (Figure 2*A*). Similarly, the expression of p-mTOR and pSTAT1 was repressed significantly in CH-C livers with a low Fischer's ratio compared with those with a high Fischer's ratio (Supplementary Figure 2, Supplementary Table 2).

To examine whether decreased pSTAT1 expression might be owing to repressed mTORC1 signaling, we knocked down the expression of Raptor, a specific subunit of mTORC1. We achieved more than 50% knockdown of Raptor by specific siRNA (Figure 2*B*). Under these conditions, the expression of p-mTOR and pSK6 were repressed, which is consistent with previous reports.[16] The expression of pSTAT1 also was repressed after Raptor knockdown (Figure 2*B*).

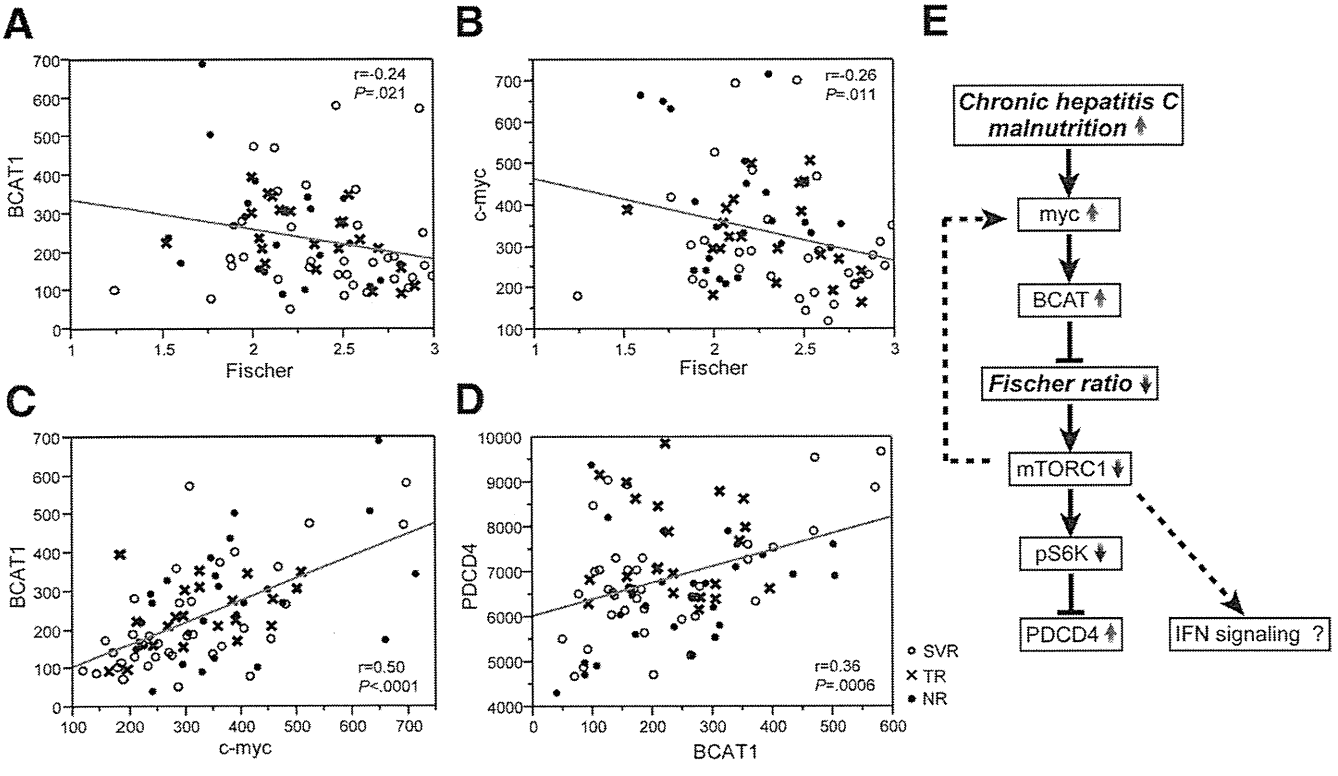

Figure 1. Regression analysis of mTORC1-related gene expression in liver. Gene expression values were determined by probe intensities. (*A*) BCAT1 and Fischer's ratio. (*B*) c-myc and Fischer's ratio. (*C*) BCAT1 and c-myc. (*D*) PDCD4 and BCAT1. (*E*) Putative signaling of mTORC1-related genes in CH-C.

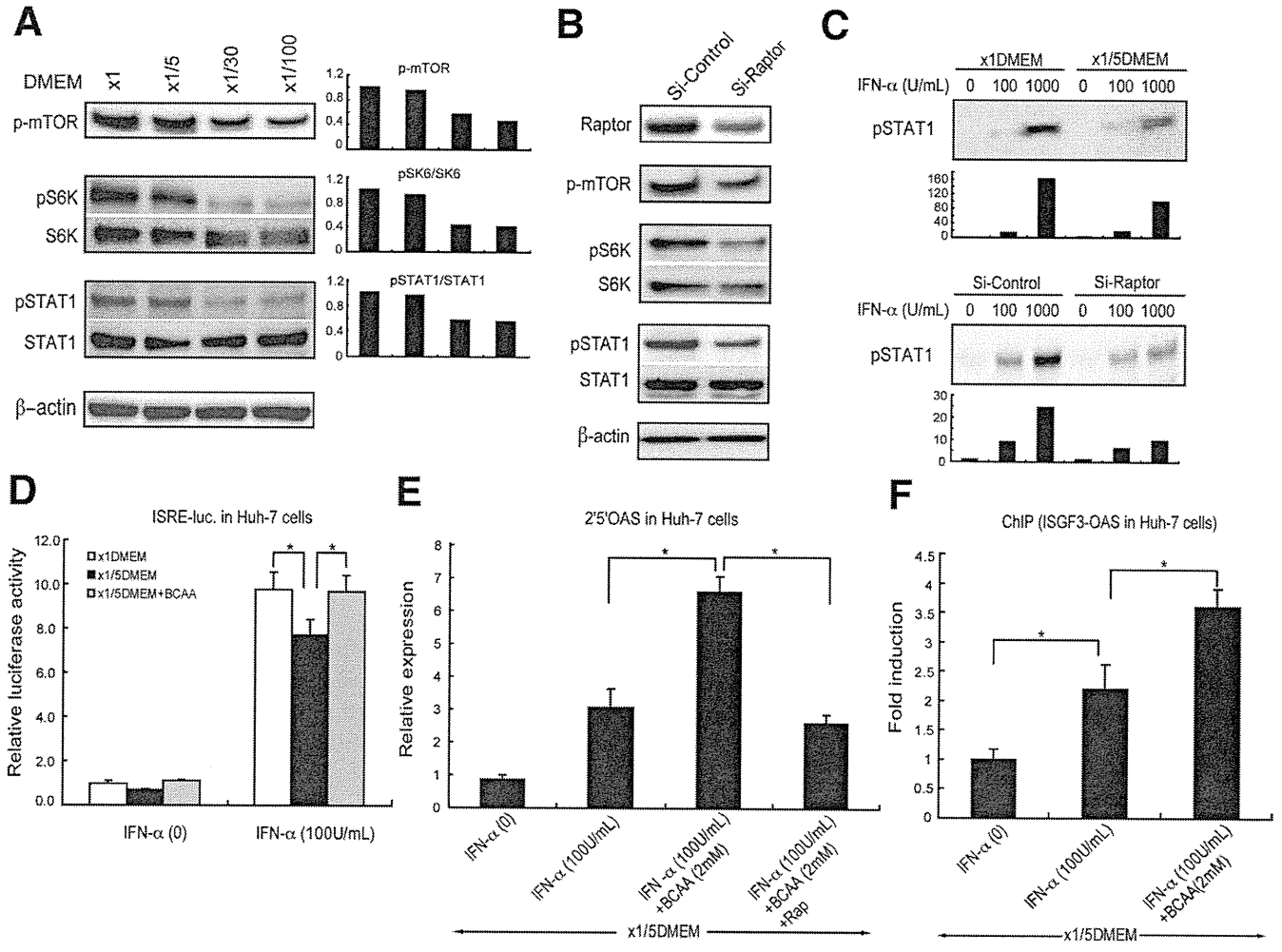

Figure 2. mTORC1 and IFN signaling in Huh-7 cells in low-amino-acid medium. (*A*) p-mTOR, pS6K, and pSTAT1 expression in different amino acid media. (*B*) p-mTOR, pS6K, and pSTAT1 expression under Raptor knock-down conditions. (*C*) IFN-alfa stimulation and pSTAT1 expression in low-amino-acid media or under Raptor knock-down conditions. (*D*) IFN-alfa stimulation and ISRE reporter activities in normal and low-amino-acid media. (*E*) IFN-alfa stimulation and 2'5'OAS expression supplemented with BCAA or rapamycin in low-amino-acid medium. (*F*) Chromatin immunoprecipitation of 2'5'OAS promoter region by ISGF3γ.

The induction of pSTAT1 by IFN-alfa (1000 U/mL) stimulation was impaired in ×1/5 DMEM or in Raptor knocked-down condition, compared with the control (Figure 2*C*). Consistent with these results, IFN-alfa–induced ISRE-dependent transcriptional activity, as measured using an ISRE-luciferase reporter assay, was impaired significantly in ×1/5 DMEM compared with ×1 DMEM (Figure 2*D*). However, this activity could be rescued by the addition of 2 mmol/L BCAA (Figure 2*D*). These results were confirmed by determining the expression of the endogenous IFN-alfa responsive gene, 2'5'OAS, using quantitative reverse-transcription PCR. Figure 2*E* shows that BCAA treatment augmented 2'5'OAS expression in low levels of amino acids, and that this could be reversed by the addition of rapamycin, an inhibitor of mTORC1 (Figure 2*E*). Furthermore, chromatin immunoprecipitation (ChIP) experiments revealed that transcriptional augmentation by BCAA was mediated by the binding of the IFN-alfa–inducible transcription factor, ISGF3γ, to the promoter region of 2'5'OAS (Figure 2*F*). These results indicate that amino acids in culture media play an essential role in IFN-alfa signaling through mTORC1 signaling, and that the addition of BCAA can overcome impaired IFN-alfa signaling in Huh-7 cells.

Induction of Socs3 in Low-Amino-Acid Medium in Huh-7 Cells

Besides being involved in mTOR signaling, Foxo transcriptional factors mediate another important branch of nutrition-sensing signaling pathway.[17] Therefore, we evaluated forkhead box O3A (Foxo3a) expression in low-amino-acid conditions in Huh-7 cells. After 6 hours culture in ×1/5, ×1/30, and ×1/100 DMEM, expression of the phosphorylated form of Foxo3a (pFoxo3a) decreased, whereas that of total Foxo3a increased in ×1/5 and ×1/30 DMEM, and the ratio of pFoxo3a to Foxo3a (pFoxo3a/Foxo3a) substantially decreased (Figure 3*A* and *B*). It has been reported that dephosphorylated Foxo3a is translocated to the nucleus before activation of its target genes.[18] In the present study, immunofluorescent staining

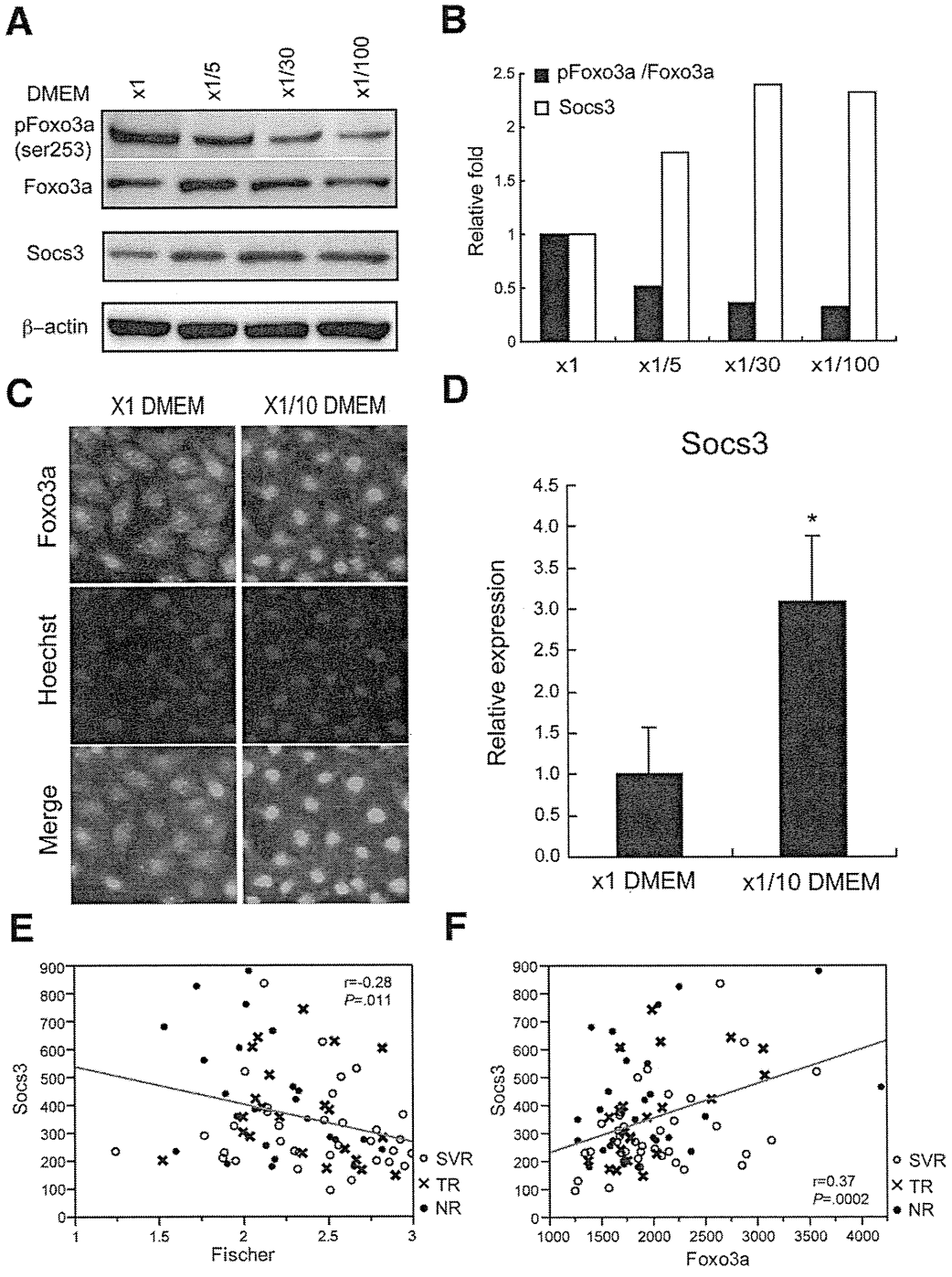

Figure 3. Foxo3a and Socs3 signaling in Huh-7 cells in low-amino-acid medium. (*A*) Foxo3a and Socs3 expression in different amino acid media. (*B*) Relative change of pFoxo3a/Foxo3a and Socs3 expression in different amino acid media. (*C*) Immunofluorescence staining of Foxo3a in Huh-7 cells in normal and low-amino-acid media. (*D*) Relative change of Socs3 messenger RNA in Huh-7 cells in normal and low-amino-acid media. (*E*) Regression analysis of Socs3 in liver and Fischer's ratio. (*F*) Regression analysis of Socs3 and Foxo3a in liver.

with an anti-Foxo3a antibody showed that Foxo3a diffused in both the cytoplasm and nucleus in normal amino acid medium, but localized in the nucleus in low-amino-acid medium (×1/10 DMEM) (Figure 3*C*).

Interestingly, in low-amino-acid medium, transcription and protein expression of Socs3 increased significantly (Figure 3*A*, *B*, and *D*). The induction of Socs3 in a state of malnutrition also was confirmed in clinical samples. In CH-C livers there was a significant negative correlation between the plasma Fischer's ratio and Socs3 expression, implying that Socs3 expression increases during the malnutrition state induced by CH-C. There was also a significant correlation between Foxo3a and the transcriptional level of Socs3 in CH-C livers (Figure 3*E* and *F*), suggesting an in vitro and in vivo biological role for Foxo3a in the activation of Socs3 expression. These findings also were confirmed by Western blotting of CH-C livers (Supplementary Figure 2, Supplementary Table 2).